

STUDY OF ENHANCED OIL RECOVERY BY  
LIQUID CARBON DIOXIDE INJECTION

FIKRI IRAWAN

MASTER OF SCIENCE  
DEPARTMENT OF PETROLEUM ENGINEERING  
UNIVERSITI TEKNOLOGI PETRONAS

MAY 2010



## STATUS OF THESIS

Title of thesis

Study of Enhanced Oil Recovery by Liquid Carbon Dioxide Injection

I FIKRI IRAWAN

hereby allow my thesis to be placed at the Information Resource Center (IRC) of Universiti Teknologi PETRONAS (UTP) with following conditions:

1. The thesis becomes the property of UTP.
2. The IRC of UTP may take copies of the thesis for academic purpose only.
3. The thesis is classified as:

Confidential

Non-Confidential

If this thesis is confidential, please state the reason:

---

The contents of the thesis will remain confidential for \_\_\_\_\_ years.

Remark on disclosure:

---

Endorsed by

---

Jl. Nusantara 1 No.56 RT3/RW13,  
Duri, Riau,  
INDONESIA, 28884

---

DR SONNY IRAWAN

Department of Petroleum Engineering  
Universiti Teknologi PETRONAS,  
Seri Iskandar, Tronoh, Perak,  
MALAYSIA, 31750

UNIVERSITI TEKNOLOGI PETRONAS  
STUDY OF ENHANCED OIL RECOVERY BY  
LIQUID CARBON DIOXIDE INJECTION

by

FIKRI IRAWAN

The undersigned certify that they have read, and recommended to the Postgraduate Studies Programme for acceptance this thesis for the fulfillment of the requirements for the degree stated.

Signature: \_\_\_\_\_

Main Supervisor: Dr Sonny Irawan

Signature: \_\_\_\_\_

Co-Supervisor: \_\_\_\_\_

Signature: \_\_\_\_\_

Head of Department: AP Ir Abdul Aziz Omar CEng FIChem

Date: \_\_\_\_\_

STUDY OF ENHANCED OIL RECOVERY BY  
LIQUID CARBON DIOXIDE INJECTION

by

FIKRI IRAWAN

A Thesis

Submitted to the Postgraduates Study Programme

as a Requirement for the Degree of

MASTER OF SCIENCE

PETROLEUM ENGINEERING PROGRAMME

UNIVERSITI TEKNOLOGI PETRONAS

BANDAR SERI ISKANDAR,

PERAK

JANUARY, 2010

## DECLARATION OF THESIS

Title of thesis

Study of Enhanced Oil Recovery by Liquid Carbon Dioxide Injection

I FIKRI IRAWAN

hereby declare that the thesis is based on my original work except for quotations and citations which have been duly acknowledged. I also declare that it has not been previously or concurrently submitted for any other degree at UTP or other institutions.

Witnessed by

\_\_\_\_\_  
Jl.Nusantara 1 No.56 RT3/RW13 Duri,  
Riau, INDONESIA, 28884

\_\_\_\_\_  
DR SONNY IRAWAN

Date : \_\_\_\_\_

Date : \_\_\_\_\_

## **DEDICATION**

Praise eternally is entirely and exclusively for Allah, the only God of all known universe,

This Thesis is dedicated to my beloved

Dad, who kept holding my hand whenever I fell,

Mom, the best mother in the world who always believe in me, and

Ria, Putri, Beril, the three future diamonds.

## **ACKNOWLEDGEMENT**

I would like to thank Allah subhanahu wata'alaah and Muhammad shallalallaahu 'alaihi wasallam.

First and foremost, I would like to thank my Research Supervisor the honorable Dr Sonny Irawan and my former Supervisor Prof Mariyamni Awang for their guidance during my research project. I would like to thank Mr. Hilfan Khairi for providing some significant materials to support this study. Also thank you to Universiti Teknologi PETRONAS for providing well-equipped facilities to conduct this research.

Many thanks to my family and friends who support me to pursue my Master Degree. The unforgettable UKM '03, for all the joy and colorful days that brought me this far.

This work could not have been possible without the advice and support of so many people.

## ABSTRACT

Typical high residual oil saturation after primary and secondary recovery encourages the application of EOR methods. Especially in a mature field with less force from its driving mechanisms due to the nature of the reservoir when it was discovered or even after long time of production. Based on literature study, CO<sub>2</sub> injection has been an excellent solvent for EOR because of its miscibility ability with crude oil at lower pressure compared to other gases such as Nitrogen and Hydrocarbon gases. However, the injection of CO<sub>2</sub> in gas state stimulates the occurrence of early gas breakthrough at the producer due to fingering phenomena.

The objective of this study is to investigate oil recovery by liquid CO<sub>2</sub> injection as EOR displacement fluid. Additional study on Interfacial Tension between CO<sub>2</sub> and the crude oil was conducted and the Minimum Miscibility Pressure was estimated by using the combination of Lasater and Holm-Josendal correlation. Berea Sandstone core plug and one of Malaysian basin light crude oil was used as experiment sample in this study. Oil recovery was generated by core flooding test to collect the produced oil during core displacement.

From the results of the experiments, it is concluded that oil recovery by water floods were in such limit of 36.6% until 38% after injecting 9 PV of water. Meanwhile, the results of CO<sub>2</sub> injection in this study gave various and interesting recovery over the residual oil in place with range of 24.7% until 72.6% depend on inlet pressures (950-1500 psig) and injection temperatures (5-20°C) of CO<sub>2</sub>. The cumulative oil recovery was recorded after injecting 10 PV of liquid CO<sub>2</sub>.

## ABSTRAK

Kandungan sisa minyak yang banyak selepas pemulihan primer and sekunder telah mendorong kepada aplikasi EOR. Terutamanya untuk telaga tua yang sudah beroperasi untuk sekian lama. Kajian sastera menunjukkan bahawa injeksi CO<sub>2</sub> merupakan pelarut unggul untuk aplikasi EOR kerana berupaya untuk melarutkan minyak pada tekanan jika dibanding dengan gas Nitrogen dan gas Hidrokarbon. Namun, disebabkan fenomena *fingering*, injeksi CO<sub>2</sub> telah mengakibatkan penerobosan gas yang terlampau awal.

Tujuan kajian ini adalah mengkaji pemulihan minyak dengan menggunakan CO<sub>2</sub> sebagai secair pemindahan dalam EOR. Penyelidikan ketegangan antara muka CO<sub>2</sub> dan minyak telah dijalankan. Tekanan minima untuk CO<sub>2</sub> larut dalam minyak telah dianggar dengan mengabungkan korelasi Lasater dan Holm-Josendal. Teras plag dari Berea Sandstone dan minyak mentah ringan dari cekungan Malaysia digunakan sebagai sampel percubaan dalam kajian ini. Pemulihan minyak diperoleh daripada ujian banjir teras.

Kajian menunjukkan pemulihan oleh banjir air dalam batasan 36.6% hingga 38% selepas menyuntik 9 PV air. Sementara itu, bergantung pada tekanan masuk (950-1500 psig) dan suhu injeksi (5-20 °C) CO<sub>2</sub>, pemulihan atas sisa minyak di tempat adalah antara 24.7% hingga 72.6%. Pemulihan minyak kumulatif dicatat selepas menyuntik 10 PV CO<sub>2</sub> cair.

In compliance with the terms of the Copyright Act 1987 and the IP Policy of the university, the copyright of this thesis has been reassigned by the author to the legal entity of the university,

Institute of Technology PETRONAS Sdn Bhd.

Due acknowledgement shall always be made of the use of any material contained in, or derived from, this thesis.

© Fikri Irawan, 2010

Institute of Technology PETRONAS Sdn Bhd

All rights reserved.

## TABLE OF CONTENT

STATUS OF THESIS.....	i
APPROVAL PAGE .....	ii
TITLE PAGE.....	iii
DECLARATION OF THESIS .....	iv
DEDICATION.....	v
ACKNOWLEDGEMENTS.....	vi
ABSTRACT.....	vii
COPYRIGHT PAGE .....	ix
TABLE OF CONTENT.....	x
LIST OF TABLES.....	xiv
LIST OF FIGURES .....	xv
LIST OF SYMBOLS .....	xviii
CHAPTER 1 INTRODUCTION.....	1
1.1 Background.....	1
1.2 Carbon Dioxide Flooding.....	2
1.3 Problem Statement .....	3
1.4 Objectives of Research.....	5
1.5 Scope of Research .....	5
CHAPTER 2 THEORY AND LITERATURE REVIEW .....	7

2.1	Enhanced Oil Recovery.....	7
2.2	Interfacial Tension.....	8
2.3	CO <sub>2</sub> Displacement.....	12
2.3.1	Vaporization of Hydrocarbons by CO <sub>2</sub> .....	12
2.3.2	Mechanisms for CO <sub>2</sub> Miscibility with Oil.....	12
2.3.3	Determination of Thermodynamic MMP.....	13
2.3.4	Estimation of Thermodynamic MMP with correlation.....	15
2.4	Effect of Injection Pressures on CO <sub>2</sub> Flood Oil Recovery.....	18
2.5	CO <sub>2</sub> Fluid Properties.....	19
2.6	Mobility and Mobility Ratio.....	21
2.7	Previous Study of CO <sub>2</sub> Enhanced Oil Recovery.....	23
CHAPTER 3 RESEARCH METHODOLOGY.....		27
3.1	CO <sub>2</sub> -Crude Oil IFT Measurement.....	28
3.1.1	Flowchart Diagram of IFT Measurement.....	28
3.1.2	IFT Measurement Apparatus.....	29
3.2	MMP Estimation.....	30
3.3	Core Flood Test.....	31
3.3.1	Flowchart Diagram of Core Flood Test.....	31
3.3.2	Porosity Measurement.....	33
3.3.3	Density Measurement.....	33
3.3.4	Initial Core Saturation.....	34

3.3.5	Core Flood Test Apparatus .....	35
3.3.6	Core Sample Cleaning .....	37
CHAPTER 4 RESULTS AND DISCUSSIONS.....		39
4.1	MMP Estimation by Using the Combination of Lasater and Holm-Josendal Correlation.....	39
4.2	Effect of CO <sub>2</sub> injection to Oil Recovery on Core Flood Tests.....	41
4.2.1	Porosity Measurement Results.....	41
4.2.2	Core Flood Experiment Results .....	41
4.2.3	Mobility Ratio Calculations .....	49
4.2.4	Continuous Gas CO <sub>2</sub> Injection.....	51
4.3	Measured Interfacial Tension between Crude Oil and CO <sub>2</sub> .....	53
4.4	Liquid CO <sub>2</sub> Injection Limitations.....	54
CHAPTER 5 CONCLUSIONS .....		56
CHAPTER 6 RECOMMENDATIONS.....		57
REFERENCES .....		58
APPENDIX A.....		64
APPENDIX B .....		66
APPENDIX C .....		69
APPENDIX D.....		71
APPENDIX E .....		73
APPENDIX F.....		75
APPENDIX G.....		77

APPENDIX H.....83

## LIST OF TABLES

Table 2.1 IFT Values in Water-Methane System. [32].....	10
Table 2.2 IFT values in oil-gas CO <sub>2</sub> system. [34].....	10
Table 2.3 Specification range of Slim-Tube equipment. [38] .....	14
Table 2.4 Physical Properties of CO <sub>2</sub> . [46].....	20
Table 2.5 Summary of Selected CO <sub>2</sub> Miscible Flood Projects. [15] .....	24
Table 3.1 Summary of injection procedures for core flood tests. ....	38
Table 4.1 Calculation summary of estimating MMP.....	40
Table 4.2 Porosity measurement results of Berea Sandstone by using PoroPerm.....	41
Table 4.3 Core flood injection profile and oil recovery.....	42
Table 4.4 CO <sub>2</sub> Viscosity properties at several pressures and temperatures in this study. (after Jarrel et.al [26]) .....	49
Table 4.5 Mobility Ratio calculation results at liquid CO <sub>2</sub> condition.....	50
Table 4.6 Core flood injection profile and oil recovery by Continuous Gas CO <sub>2</sub> injection.....	52
Table 4.7 IFT values measured between crude oil sample and CO <sub>2</sub> at different equilibrium pressures. ....	53

## LIST OF FIGURES

Figure 2.1 The dependence of residual oil saturation on capillary number. [10] .....	9
Figure 2.2 Methane-water interfacial tension. [35] .....	11
Figure 2.3 IFT Measurement by using pendant drop method.....	11
Figure 2.4 Slim Tube equipment schematic. [38].....	14
Figure 2.5 Thermodynamic MMP Prediction by Holm & Josendal with Mungan Extended. [44].....	16
Figure 2.6 Relationship between $C_{5+}$ Effective Molecular Weight and API Degree of crude oil. [40].....	17
Figure 2.7 Slim tube miscibility test. [21] .....	19
Figure 2.8 Phase Diagram of pure $CO_2$ . [26].....	21
Figure 2.9 Oil fields producing from formations with $T_f$ less than $T_{cCO_2}$ and initial pressure greater than the saturation pressure of $CO_2$ at that formations temperature. [48].....	25
Figure 3.1 Research methodology flowchart diagram.....	27
Figure 3.2 Flow Diagram of IFT measurement. ....	28
Figure 3.3 Schematic Diagram of IFT-700.....	29
Figure 3.4 A Camera and High Pressure Cell on IFT-700. ....	30
Figure 3.5 Flow Diagram of $CO_2$ Core Flooding Experiment. ....	32
Figure 3.6 PoroPerm equipment to measure core porosity.....	33
Figure 3.7 Portable Density Meter equipment to measure liquid density.....	34
Figure 3.8 Manual Saturator for core sample initial saturation. ....	35

Figure 3.9 Smart Series Software <sup>TM</sup> Interface on RPS-830 Relative Permeability Test Equipment. ....	35
Figure 3.10 Schematic diagram of the experimental set-up for Core Flooding.....	36
Figure 3.11 Water Bath for CO <sub>2</sub> temperature conditioning. ....	36
Figure 3.12 Panels to operate RPS-830. ....	37
Figure 3.13 Soxlet Extractor for core cleaning by using Toluene as Cleaning Agent.	38
Figure 4.1 Oil recovery as effect of liquid CO <sub>2</sub> injection at various pressures and temperatures of CO <sub>2</sub> injected. ....	42
Figure 4.2 Oil recovery as effect of CO <sub>2</sub> injection at 950 psig.....	44
Figure 4.3 Oil recovery as effect of CO <sub>2</sub> injection at 1200 psig.....	44
Figure 4.4 Oil recovery as effect of CO <sub>2</sub> injection at 1500 psig.....	45
Figure 4.5 Oil recovery at constant CO <sub>2</sub> temperature of $T = 20^{\circ}\text{C}$ and various injection pressure. ....	46
Figure 4.6 Oil recovery at constant injection pressure of $P = 950$ psig and various injected CO <sub>2</sub> temperature.....	46
Figure 4.7 Oil recovery at constant CO <sub>2</sub> temperature of $T = 12^{\circ}\text{C}$ and various injection pressure. ....	47
Figure 4.8 Oil recovery at constant injection pressure of $P = 1200$ psig and various injected CO <sub>2</sub> temperature.....	47
Figure 4.9 Oil recovery at constant CO <sub>2</sub> temperature of $T = 5^{\circ}\text{C}$ and various injection pressure. ....	48
Figure 4.10 Oil recovery at constant injection pressure of $P = 1500$ psig and various injected CO <sub>2</sub> temperature.....	48
Figure 4.11 Cumulative oil recovery by injecting Gas CO <sub>2</sub> at 1500 psig and 40°C....	51

Figure 4.12 Measured interfacial tension of crude oil-CO<sub>2</sub> system at various pressure  
and  $T = 25^{\circ}\text{C}$ . .....53

## LIST OF SYMBOLS

### *Notations*

$d_e$	Equatorial diameter, m
$d_s$	Diameter of the drop at the height $d_e$ above the bottom of drop, m
$f$	Drop shape factor, ratio of $d_s/d_e$ , dimensionless
$g$	Gravity acceleration, $m/s^2$
$k_i$	Effective permeability of phase $i$ , md
$M$	Mobility ratio, dimensionless
$p$	Reservoir pressure, psia
$S_{orw}$	Oil residual saturation after water flood, fraction of pore volume
$S_{wc}$	Connate water saturation after crude oil injection, fraction of pore volume
$T$	Reservoir temperature, °F
$T_f$	Formation Temperature, °F
$T_{ccO_2}$	CO <sub>2</sub> critical temperature, °F
$u_i$	Superficial (Darcy) velocity of phase $i$ , D/ft <sup>2</sup>
$V_b$	Bulk Volume, ml
$V_g$	Grain Volume, ml
$V_p$	Pore Volume, ml
$x$	Distance, m

### *Greek Symbols*

$\gamma$	Oil Specific Gravity, dimensionless
$\lambda_i$	Mobility of phase $i$ , md/cp
$\lambda_D$	Mobility of the displacing fluid phase, md/cp
$\lambda_d$	Mobility of the displaced fluid phase, md/cp
$\mu_i$	Viscosity of phase $i$ , cp
$\mu_d$	Viscosity of the displaced fluid phase, md/cp
$\mu_D$	Viscosity of the displacing fluid phase, md/cp
$\phi$	Porosity, fraction
$\rho^L$	Liquid phase density, kg/m <sup>3</sup>
$\rho^V$	Vapor phase density, kg/m <sup>3</sup>
$\rho_o$	Oil density at standard condition, g/cm <sup>3</sup>
$\rho_w$	Water density at standard condition, g/cm <sup>3</sup>
$\sigma$	Interfacial tension, mN/m

## CHAPTER 1

### INTRODUCTION

#### 1.1 Background

Most oil reservoir bear to a period called primary recovery after discovery. Typical residual oil saturation in light or medium oil reservoir is in the range of 20-50% of the Original Oil in Place (OOIP) during this period of production [1] [2] [3]. This natural energy will dissipate eventually due to production period or problems in reservoir. When this happens, external energy must be added to the reservoir to produce the remaining oil. This method is known as Enhanced Oil Recovery (EOR). In Malaysia, the total proven oil reserves until September 2009 is 4 billion barrels which is based on 68 oil fields including 7 new fields that had come online in 2008 [4]. If only the optimum recovery could be acquired by primary production, it means there are 2 billion barrels of oil will be the primary target for EOR. On top of that value, most of the fields are already moving into mature stage for primary and secondary depletion [5]. This situation will further merit the application of EOR processes.

Capillary force which occur because of Interfacial Tension (IFT) that happens between two different and immiscible fluid is one of the important factors that cause a large amount of the original oil in place not to be recovered by water flooding [6] [7].

Different EOR techniques have been widely applied to recover the residual oil after water flood. These techniques become increasingly important to the petroleum industry. Basically, the EOR techniques for the light oil reservoirs include chemical method and solvent injection methods. The common chemical EOR processes are Alkaline, Surfactant and Polymer (ASP) flooding. Both the alkaline and surfactant

flooding processes are based on the similar mechanism, such as the IFT reduction between the injected fluid and the reservoir fluid to low or ultra-low values [8] [9]. In this case, the capillary force is greatly reduced so that higher oil recovery could be achieved. In the polymer flooding, polymers are added into the injected fluid at low concentrations to increase the viscosity of the injected fluid. Therefore, polymer flooding helps to prevent or reduce the early breakthrough of the injected fluid consequently, the sweep efficiency is improved and the oil recovery is enhanced.

In EOR methods by solvent injection, for non hydrocarbon solvent (e.g. carbon dioxide, flue gas, carbon monoxide, air, and nitrogen) or hydrocarbon solvents (e.g. natural gas, methane, ethane, propane, butane, liquefied natural gas, and liquefied petroleum gas), are directly injected into the reservoir continuously or intermittent. Two different displacement cases, namely miscible and immiscible flooding, can occur when a solvent is injected into a reservoir. In the miscible flooding processes, the injected solvent and the crude oil reservoir mixed together in any proportions and all the mixture remains in a single phase [10]. In this case, the IFT between the crude oil and the injected solvent is reduced until approaching zero and consequently the capillary force is very low. As a result, the residual oil saturation is greatly reduced.

## **1.2 Carbon Dioxide Flooding**

In the 1950's, petroleum industry began to carry out gas-injection projects in search of a miscible process that would recover oil effectively for EOR purposes [11]. Among the EOR methods for the light and medium oil reservoirs, carbon dioxide flooding had been successful to a large extent under some favorable reservoir conditions [10] [12]. It is sensible to underline that CO<sub>2</sub> EOR method not only effective in enhancing oil recovery but also considerably reduces greenhouse gas emissions [13] [14]. In the past five decades, there have been laboratory studies, numerical simulations and field applications of CO<sub>2</sub> EOR processes. In general, it has been found that these tertiary processes could recover various range of oil recovery [15] [16] [17]. In addition, this study is intended to augment the comprehension and understanding about CO<sub>2</sub> injection generally and liquid CO<sub>2</sub> injection exclusively by way of analyzing the core flood experiment results and IFT measurement.

Successful CO<sub>2</sub> flooding is largely controlled by the interactions between the injected CO<sub>2</sub> and the reservoir crude oil. These interactions determine the overall performance of the CO<sub>2</sub> EOR process. For example, when CO<sub>2</sub> is injected into an oil reservoir at high reservoir pressure, the IFT between crude oil and CO<sub>2</sub> is significantly reduced. The reduction in IFT increases the viscous force to capillary force ratio and thus lowers the residual oil saturation. In addition, the oil and CO<sub>2</sub> relative permeability also depend on the IFT between the crude oil and CO<sub>2</sub> [10] [18].

In order to have an effective CO<sub>2</sub> flood, a CO<sub>2</sub>-hydrocarbon miscible solvent bank has to be formed and maintained to maximize displacement. The introduction of water in WAG process delays this mechanism and severely reduces displacement efficiency [19].

### 1.3 Problem Statement

Gas injection alone decreases the residual oil saturation in the reservoir significantly. Gas has lower density and higher mobility therefore it could easily sweep the oil parts in the attic parts of the reservoir. Gas injection has major problems associated with it such as early breakthrough due to fingering. This will cause shorter contact time with crude oil in the reservoirs. Continuous Gas CO<sub>2</sub> injection was poor in areal sweep efficiency which resulted in early breakthrough. Previous studies also indicated that the production Gas Oil Ratio (GOR) for continuous gas CO<sub>2</sub> injection was very high [20].

The introduction of water in WAG process delays hydrocarbon-CO<sub>2</sub> bank establishment and reduces displacement efficiency [19] [21]. Laboratory experiment verified that simultaneous injection of solvent and water into water flooded core results in trapping of both oil and solvent. Experiments using Berea cores demonstrated that WAG ratio between 1 and 3 severely reduced oil recovery. Upon imbibitions of water, oil was trapped over a range of saturation. Raimondi and Torcasso [22] concluded that the amount oil trapped increased rapidly as the water saturation approaches the limiting value of imbibitions, i.e.,  $S_w = 1 - S_{or}$ . The result of this study indicated that most of the oil became trapped in the last stages of imbibitions.

Thomas and Countryman [23] mentioned that one property of a petroleum reservoir which is expected to be a major importance is the presence of interstitial water. The possible effect of interstitial water on displacement is the existing of dead-end pore in multiphase system. There are no dead-end pores at single phase system. In multiphase system, however, the second phase may entrap single pores of other phase or may even isolate fingers. Dispersion in wetting component of two immiscible liquid systems increased with decreasing saturation of the wetting fluid. This statement is concluded based on the experimental results of flowing water and oil system into Boise Sand core. The result shows that the increasing water flow rate is decreasing the advance of oil frontal on the production.

Stalkup [24] also conducted experiments of miscible displacement at high water saturation in long and consolidated of Boise, Berea, and Torpedo sandstones. The type of oil that is used in this experiment was high molecular hydrocarbon such as trimethylhexane ( $C_9$ ) and undecane ( $C_{11}$ ), and also low molecular weight hydrocarbon such as methane-*n*-butane and *i*-butane. By varying the flow rate of oil-water ratio, the experiment at different water saturation was developed. As a result, for miscible displacement in the presence of high water saturation, some of the oil was blocked by the water such that it was not able to flow and bypassed by solvent front. The results indicated that rock wettability may be an important factor that the trapping of oil by water may not be as rigorous for weakly water-wet rocks as it was in strongly water-wet laboratory sandstones.

Tiffin and Yellig [25] reported that in water-wet EOR tests, water injected simultaneously with  $CO_2$  entraps significant amount of oil. Lower oil recovery was resulted during the development of miscibility. This condition happened because of water shielding portions of oil from the injected  $CO_2$ . As more water was injected, more oil entrapped and oil recovery decreased. It was evident that oil recovery related to the rate at which  $CO_2$  could diffuse through the water and displace the trapped oil. Lower injection rate allowed more time for the  $CO_2$  to diffuse through the water and displace the trapped oil.

Based on the above studies, it is important to find another alternative on tertiary recovery that could develop miscibility between CO<sub>2</sub> and crude oil while maintaining mobility in the reservoir with better sweep efficiency without facing any water blocking problems. The method proposed in this study is to use CO<sub>2</sub> in liquid state as the solvent injected to displace residual oil in the reservoir.

#### **1.4 Objectives of Research**

The research objectives of this study are as follows:

1. To measure the Interfacial Tension between crude oil sample and CO<sub>2</sub>.
2. To estimate the Minimum Miscibility Pressure of CO<sub>2</sub> flooding experiment.
3. To conduct liquid CO<sub>2</sub> core flood experiment and measure the oil recovery.

#### **1.5 Scope of Research**

This research concentrates on investigating the potential of liquid CO<sub>2</sub> as an EOR method by means of Berea Sandstone core and one of Malaysian light crude oil as sample. Before core flooding, the IFT measurement between CO<sub>2</sub> and crude oil will be conducted for analysis of the effect of various equilibrium pressures at constant temperature of flooding experiment. The IFT measurement will proceed at different pressure ranging from 400 psig until 1500 psig and temperature of 25°C. The temperature of 25°C is selected because the core flood experiment will be conducted at this temperature. Meanwhile, the measurement pressure range previously is selected because the core flood inlet pressures are within this value. This pressure is also selected to observe the effect of various equilibrium pressures to the IFT between crude oil and CO<sub>2</sub>. Pendant drop method is used in this experiment because the density of crude oil is higher compared to the density of CO<sub>2</sub> along for all measurement conditions. Every pressure conditions will require 10 minutes of measurement period with one second of recording interval.

Prior to core flood laboratory experiment, the minimum miscibility pressure of CO<sub>2</sub>-crude oil system will be estimated by using the combination of Lasater and Holm-

Josendal correlations to ensure that the experiment is conducted above the miscibility condition.

Core flooding process will be conducted at three different inlet pressures of 950 psig, 1200 psig, and 1500 psig. For each pressure, the temperature of CO<sub>2</sub> injected will be varied in 5°C, 12°C, and 20°C. At these conditions, the CO<sub>2</sub> injected will be in liquid phase based on the existing CO<sub>2</sub> phase behavior data [26]. The core sample will be retained at temperature of 25°C during core flood experiment to represent the core temperature.

Three fresh Berea sandstones have been prepared for core flooding experiment and one of Malaysian basin light crude oil as the oil sample. The dimension of these core samples are 3 inches length and 1.5 inches in diameter. Prior measurement of crude oil density and viscosity will be conducted for the purpose of knowing the classification of crude oil employed. Core porosity will be measured by using PoroPerm equipment which occupies Nitrogen as the confining pressure and Helium for porosity measurement. Flooding experiment will utilize Temco RPS-830 HTHP Relative Permeability Test System.

## CHAPTER 2

### THEORY AND LITERATURE REVIEW

#### 2.1 Enhanced Oil Recovery

Enhanced Oil Recovery (EOR) is methods to recover crude oil by the injection of materials not normally present in the reservoir. This definition covers all modes of oil recovery processes (drive, push-pull, and well treatments) and most oil recovery agents. After the natural energy is depleted, hydrocarbon production will declines and a secondary phase of a production begin when supplemental energy is added to the reservoir by injection of water. As the produced Water-Oil Ratio (WOR) of the field approaches an economic limit of operation and the net profit is decreasing due to the differences between the value of produced oil and the cost of water treatment, the tertiary period of production begins. Since this last period in the history of the field commences with the introduction of solvents, chemical, or thermal energy to enhance oil production, it has been labeled as EOR. However, EOR may be initiated at any time during the history of an oil reservoir when it become obvious that some type of chemical or thermal energy must be used to stimulate production [27].

General classification of EOR methods are explained as follow [28]:

1. Chemical EOR are characterized by the addition of chemicals into water in order to reduce the mobility of displacing agent and/or lowering the IFT. The basic principle of this method is the improvement of sweep efficiency and displacement efficiency.

2. Miscible gas methods have their greatest potential for EOR of low-viscosity oils. These processes are mainly in reducing the IFT to improve displacement efficiency. Among these methods, hydrocarbon gas (LPG, alcohol), nitrogen and CO<sub>2</sub> miscible flooding on a large scale is expected to make the greatest contribution to miscible EOR.
3. Thermal methods are for oil gravity less than 25 degree or classified as heavy oil. These processes provide a driving force and add energy (heat) to the reservoir to reduce oil viscosity and vaporize the oil.
4. Other process such as Microbial EOR, electrical heating on the reservoir, and so on.

In considering CO<sub>2</sub> feasibility, the three most important flood variables to consider are as follows [26]:

1. Significant moveable oil saturation (which depends on oil properties, remaining oil saturation, reservoir heterogeneity, and reservoir wettability).
2. The ability to achieve and maintain thermodynamic MMP in the reservoir (which depends on the average pressure, fracture parting pressure, injectivity impacts, and oil properties).
3. The ability of the CO<sub>2</sub> to contact a large portion of the reservoir including vertical, areal, and unit displacement (all of which depend on well spacing, mobility ratio, permeability, reservoir heterogeneity and geometry, injection well conformance, areal discontinuity, gas cap, and fracture system).

## **2.2 Interfacial Tension**

In dealing with multiphase system, it is necessary to consider the effect of the forces acting at the interface when two immiscible fluids are in contact. When these two fluids are liquid and gas, the interface is normally referred to the liquid surface [29]. Danesh [30] explained that IFT is a quantitative index of the molecular tension at the interface and defined as the force exerted at the interface per unit length.

One of the purposes of miscible injection is to develop very low IFT between the injected solvent and existing crude oil. As shown in Figure 2.1 that if IFT between oil and displacing fluid is reduced, thus the capillary number becomes infinite, residual oil saturation can be reduced to its lowest possible value [10].

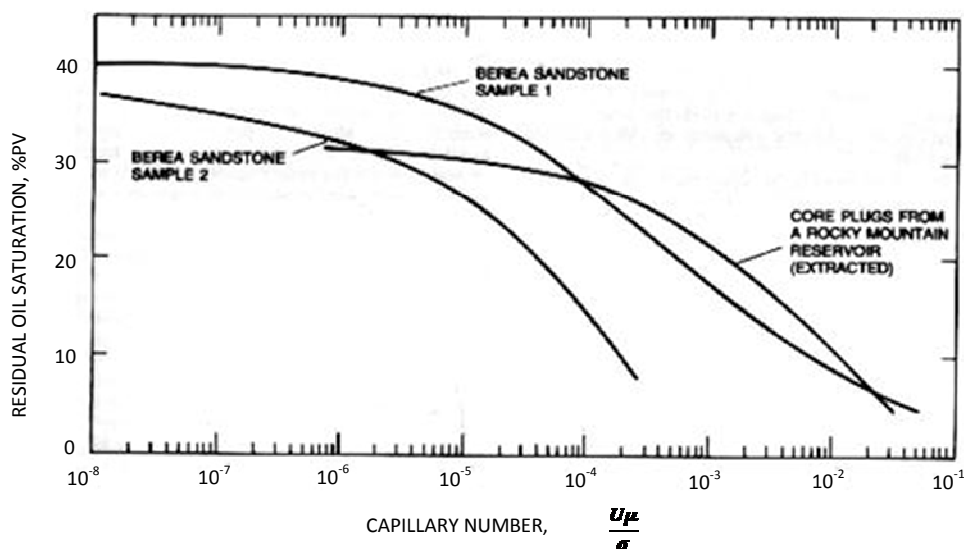


Figure 2.1 The dependence of residual oil saturation on capillary number. [10]

Here, the residual oil saturation is plotted against capillary number, the product of Darcy velocity and oil viscosity divided by IFT. Capillary number is an approximate measure of the ratio of viscous to capillary forces. Over ranges of velocity, oil viscosity, and IFT between oil and water in conventional water flooding, residual oil saturation is insensitive to capillary number [10]. Figure 2.1 shows that a drastic reduction in IFT between oil and displacing fluid is required to achieve significant reduction in residual oil saturation.

A wide variety of experimental techniques have been used in literatures for IFT measurement. Among many existing experimental methods for determining the IFT, the pendant drop method is probably the most suitable for measuring the IFT between a crude oil and test solvent at high pressures and elevated temperatures. In essence, this method determines the IFT from the drop shape analysis. The first apparatus for measuring the IFT under reservoir conditions by using the pendant drop method was established in the late 1940 [31].

Hough et.al. [32] published a result of IFT measurements for the water-methane system for 15-second-old drops, formed on a tip having diameter of 0.0472 in. The study was conducted at various pressures and temperatures as shown in Table 2.1 and showing that the IFT decreased as the temperature increased.

Table 2.1 IFT Values in Water-Methane System. [32]

Temperature (°C)	23	38	71	104	138
Pressure (psig)	IFT (mN/m)				
15	75.5	70.0	63.5	57.3	52.8
1,000	67.0	60.0	55.5	50.7	46.1
5,000	53.0	23.0	24.7	24.5	21.3
10,000	48.6	22.0	26.0	28.0	25.5
15,000	46.5	26.0	30.0	31.0	30.5

In this study, the pendant drop method has been used to measure the IFT by photographing a pendant drop and then measuring the drop dimensions from the negative film. Rao and Ayirala [33] concluded that IFT is much more strongly affected by the thermodynamic variable such as pressure, temperature, and the composition of the bulk than does the individual bulk phase properties.

Another study by Kechut et.al. [34] who compared IFT measurement by using Drop Volume Technique with previously published pendant drop method was showing that at temperature 77°C, the IFT of crude oil taken from stock tank with CO<sub>2</sub> gas decreases with the increasing equilibrium pressure. The result of this experiment is shown in Table 2.2.

Table 2.2 IFT values in oil-gas CO<sub>2</sub> system. [34]

Pressure (psig)	IFT (mN/m)	
	Drop Volume	Pendant Drop
1206	7.24	7.00
1330	5.49	5.40
1435	3.98	4.00
1515	3.53	3.50
1913	0.64	0.41

The study of Firoozabadi and Ramey [35] also reported that IFT decreased with increasing pressure and/or temperature measurement as shown in Figure 2.2.

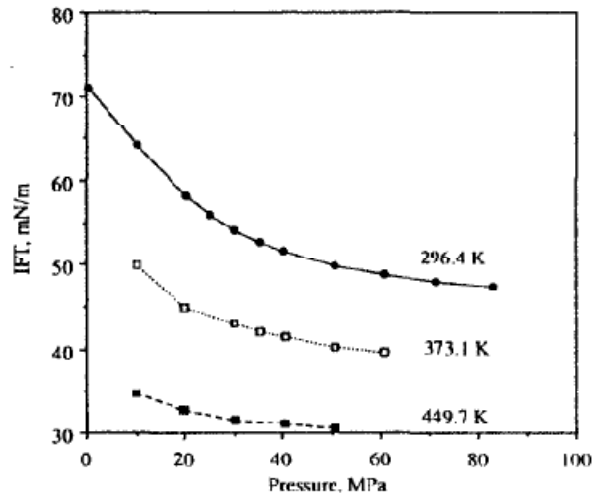


Figure 2.2 Methane-water interfacial tension. [35]

The IFT between gas and liquid at high pressure is commonly measured by using pendant drop apparatus. The shape of liquid droplet at static conditions, controlled by the balance of gravity and surface forces, is determined and related to the gas-liquid IFT [30]. The basic formula to measure the IFT with pendant drop method is displayed in Equation (1).

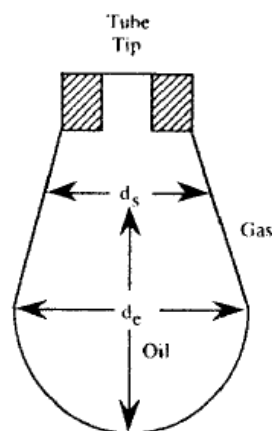


Figure 2.3 IFT Measurement by using pendant drop method.

$$\sigma = \frac{gd_e}{f}(\rho^L - \rho^V) \dots\dots\dots (1)$$

where,

$\sigma$  = interfacial tension, mN/m

$g$  = gravity acceleration, m/s<sup>2</sup>

$f$  = drop shape factor, ratio of  $d_s/d_e$ , dimensionless

$d_e$  = equatorial diameter, m

$d_s$  = diameter of the drop at the height  $d_e$  above the bottom of drop, m

$\rho^L$  = liquid phase density, kg/m<sup>3</sup>

$\rho^V$  = vapor phase density, kg/m<sup>3</sup>

## 2.3 CO<sub>2</sub> Displacement

### 2.3.1 Vaporization of Hydrocarbons by CO<sub>2</sub>

Carbon dioxide is not miscible at first contact with crude oil. However, under the right pressure, temperature, and repeated contact, carbon dioxide can vaporize certain hydrocarbons from crude oil [26]. This produces a single phase where the miscible transition zone move toward the production wells. Vaporization involves in converting the liquid into gaseous state or vapor phase. CO<sub>2</sub> can vaporize light hydrocarbon (C<sub>2</sub> – C<sub>6</sub>) and medium hydrocarbon (C<sub>7</sub> – C<sub>30</sub>), but it does not vaporize heavy hydrocarbon (C<sub>31+</sub>). However, CO<sub>2</sub> does not require the presence of light hydrocarbon components to generate miscibility unlike methane injection [36].

### 2.3.2 Mechanisms for CO<sub>2</sub> Miscibility with Oil

In general, miscibility between fluids can be achieved through two mechanisms: first-contact miscibility and multiple-contact miscibility [26] [10]. When two fluids

become miscible, they form a single phase; one fluid can completely displace the other fluid, leaving no residual saturation.

A clear example of first-contact miscibility is ethanol and water. Regardless of the proportion of the two fluids, they immediately form one phase with no observable interface [26]. Butane and crude oil also are first-contact miscible, and butane might make ideal solvents for oil were it not for its high cost. To achieve the first contact miscibility between the solvent and crude oil the pressure must be over the cricondenbar since all the solvent-oil mixtures over the pressures are single phases.

In the multiple contact miscible process that takes place between CO<sub>2</sub> and crude oils, as in this study, CO<sub>2</sub> and oil are not miscible on first contact, but require many contacts in which components of the oil and CO<sub>2</sub> transfer back and forth until the oil-enriched CO<sub>2</sub> cannot be distinguished from the CO<sub>2</sub>-enriched oil [26]. Zick [37] calls this process a condensing/vaporizing mechanism. Multiple-contact miscibility between CO<sub>2</sub> and oil starts with dense phase CO<sub>2</sub> and hydrocarbon liquid. The CO<sub>2</sub> first condenses into the oil, making it lighter and often driving methane ahead out of the “oil bank”. The lighter components of the oil then vaporize into the CO<sub>2</sub>-rich phase, making it denser, more like the oil, and thus more easily soluble in the oil [26].

### **2.3.3 Determination of Thermodynamic MMP**

The basic laboratory means of determining thermodynamic MMP is the slim-tube test, which produce 1-Dimensional displacement with a very low level of mixing. The slim tube is constructed of stainless steel, typically ¼ inch outside diameter and 40 ft long. Commonly used packing is 160 to 200 mesh Ottawa sand. The flow diagram of slim tube is shown in Figure 2.4.

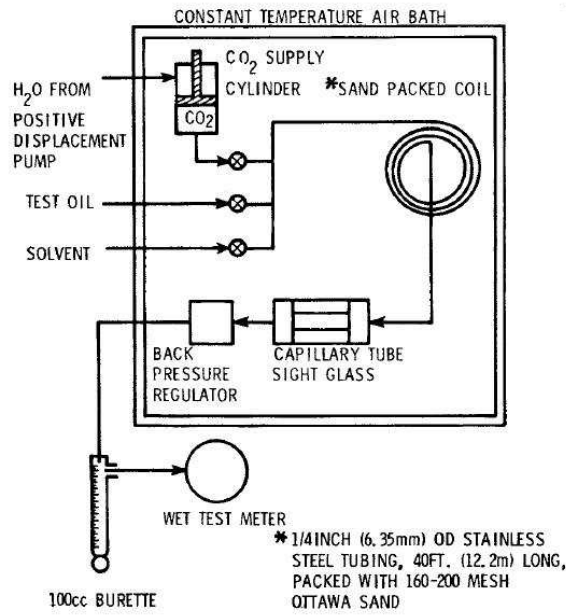


Figure 2.4 Slim Tube equipment schematic. [38]

The slim-tube method is the most common used technique for measuring the MMP between a crude oil and CO<sub>2</sub> [10] [38] [38] and has become a standard method to determine the MMP in the petroleum industry. Small diameter tube is intended to eliminate the viscous fingering effect [10] [39]. The common specification of the slim-tube apparatus was reported in the literature and shown in Table 2.3.

Table 2.3 Specification range of Slim-Tube equipment. [38]

Slim-Tube Specifications	Literature
Length (ft)	5 - 120
Inner Diameter (in.)	0.12 - 0.63
Packing Material	Glass beads, Sand, 50 mesh - 270 mesh
Porosity (%)	32 - 45
Permeability (Darcy)	2.5 - 250
Displacement Velocity (ft/D)	30 - 650

Slim tube experiment is initiated with sand pack saturation with oil at a constant temperature. Carbon dioxide is then introduced at a given pressure (controlled by a backpressure regulator), and oil displacement is measured as oil recovered. A high pressure sight glass shows the number of phases exiting the slim tube. Below the

thermodynamic MMP, the sight glass shows oils with bubbles of CO<sub>2</sub>. When the CO<sub>2</sub> has miscible with the oil, there should be essentially only one phase is flowing. The CO<sub>2</sub> displacements are carried out for a range of pressures, holding the temperature constant at the reservoir temperature. For each pressure, the oil recovery at 1.2 hydrocarbon pore volume (HCPV) of CO<sub>2</sub> injected is plotted. An oil recovery factor of at least 90% is often used as a rule of thumb for estimating thermodynamic MMP [26].

#### **2.3.4 Estimation of Thermodynamic MMP with correlation**

Determining the thermodynamic MMP with slim-tube test can be expensive [26]. The problem with conventional apparatus includes the difficulties associated with the relatively large column diameter used and the difficulties in obtaining uniform packing.

There are two possible ways to avoid slim-tube tests: mathematical models and thermodynamic correlations. Mathematical models use phase equilibrium data and an Equation of State (EOS) to estimate the thermodynamic MMP. Significant process has been made on these models in recent years, and if appropriate data are available they can yield excellent result at low cost. There are a lot of factors affecting MMP. Some of the important factors affecting MMP are oil properties, reservoir temperature, reservoir pressure, and the purity of the injected CO<sub>2</sub> because miscibility pressure is increasing with increasing of oil gravity and depth [40].

Useful thermodynamic MMP correlations have been developed by several researchers [41] [42] [43] [44]. Although the correlations have limitations and should have been used in the absence of slim-tube tests data and/or phase equilibrium data that can be input to mathematical models.

Holm and Josendal [42] determined that CO<sub>2</sub> attains dynamic miscibility with crude oil when CO<sub>2</sub> density is high enough to vaporize C<sub>5</sub>-trough-C<sub>30</sub> hydrocarbons. They found that CO<sub>2</sub> densities at the thermodynamic MMP ranged from 0.4 to 0.65 g/cm<sup>3</sup>. They also found that the thermodynamic MMP was related to the average molecular weight of C<sub>5+</sub> components of the oil, as well as to the reservoir temperature and

pressure. As shown in Figure 2.5, it is clear that heavier oil require higher pressure to become miscible. For example, at 140°F, oil with C<sub>5+</sub> molecular weight of 340 has a thermodynamic MMP above 3,000 psia. Meanwhile, the oil with lower molecular weight of 180 reaches the MMP at 2,000 psia. Figure 2.5 is also showing the extensions developed by Mungan for higher molecular weight [44].

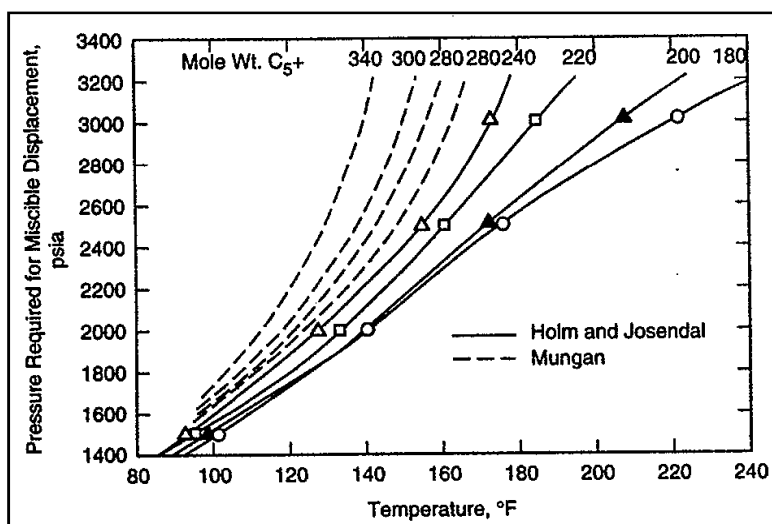


Figure 2.5 Thermodynamic MMP Prediction by Holm & Josendal with Mungan Extended. [44]

Holm and Josendal [42] conducted experiments by using 41° API crude oil in Boise sandstone with various temperatures of 71°F, 135°F, and 190°F. The resulted estimation from the above correlation resulted MMP difference in such limit of 10 psig until 150 psig below the MMP determined by using Slim Tube experiment. In this study, it is assumed that MMP estimation by using Holm and Josendal [42] is also applicable for lower temperature where the CO<sub>2</sub> is in liquid phase. This assumption is based on the trend line in Figure 2.5 where all the charts approach unity as the temperature decreases.

Holtz et.al. [40] generated an empirical correlation based on the work of Holm and Josendal to determine the MMP of CO<sub>2</sub> at various reservoir temperature and C<sub>5+</sub> component. This relationship was resulted by developing an equation through nonlinear multiple regression that allow to estimate MMP.

$$MMP = -329.558 + (7.727 * MW * 1.005^T) - (4.377 * MW) \dots\dots\dots (2)$$

where,

$MMP$  = minimum miscible pressure, psia

$MW$  =  $C_{5+}$  effective molecular weight, lb mol

$T$  = temperature reservoir, °F

A relationship between API gravity and  $C_{5+}$  molecular weight was published by Lasater [45]. As shown in Figure 2.6, Holtz et.al. [40] accomplished to developed the correlation between these two parameters as follows:

$$MW = \left( \frac{7864.9}{^{\circ}API} \right)^{\frac{1}{1.0386}} \dots\dots\dots (3)$$

where,

$MW$  =  $C_{5+}$  molecular weight, lb mol

$^{\circ}API$  = Oil API degree,  $^{\circ}API$

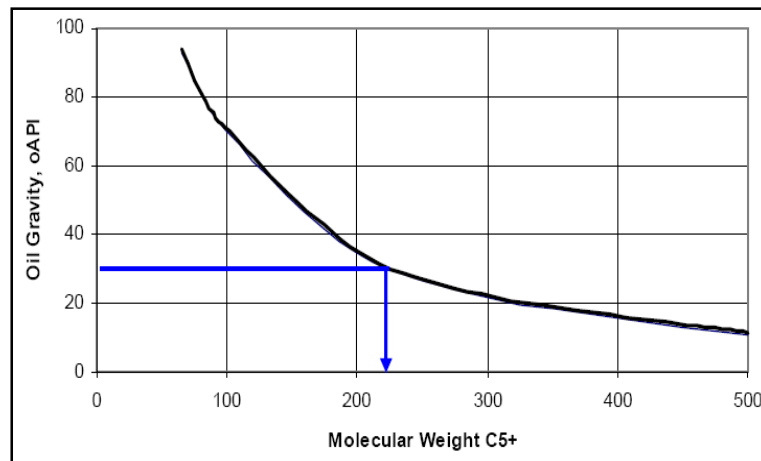


Figure 2.6 Relationship between  $C_{5+}$  Effective Molecular Weight and API Degree of crude oil. [40]

If the oil API Gravity is determined by using measurement at standard condition, atmospheric pressure 14.7 psig and temperature 15.6°C, the oil specific gravity and API° can be calculated by using Equation (4) and Equation (5) respectively.

$$\gamma = \frac{\rho_o}{\rho_w} \dots\dots\dots (4)$$

where,

$\gamma$  = Oil Specific Gravity, dimensionless

$\rho_o$  = Oil density at standard condition, g/cm<sup>3</sup>

$\rho_w$  = Water density at standard condition, g/cm<sup>3</sup>

$$^{\circ}API = \frac{141.5}{\gamma} - 131.5 \dots\dots\dots (5)$$

where,

$^{\circ}API$  = Oil API degree,  $^{\circ}API$

$\gamma$  = Oil specific gravity, dimensionless

#### 2.4 Effect of Injection Pressures on CO<sub>2</sub> Flood Oil Recovery

To significantly reduce the residual oil, carbon dioxide injection must be above the thermodynamic MMP. At lower pressure condition, the pressure is not high enough to allow sufficient CO<sub>2</sub> to dissolve into the oil or vaporize sufficient oil into the CO<sub>2</sub> so that the two phases become miscible. In this region, CO<sub>2</sub> is not dense enough and can only vaporize components up to C<sup>6</sup> [26] [42] [41]. When two immiscible phases flow simultaneously in a porous medium, the flow behavior is determined by the relative permeability characteristics of the rock. Oil relative permeability decreases with the decreasing oil saturation until it reaches a limiting value which is called the residual oil saturation. In this region, the primary effect of CO<sub>2</sub> has is to swell the oil and reduce its viscosity. Swelling causes some of the residual oil to become recoverable.

Miscibility development between CO<sub>2</sub> and oil is a function of both temperature and pressure, but for an isothermal reservoir, the only concern is pressure. Oil can dissolve more CO<sub>2</sub> as the pressure escalates and more oil component can be vaporized by the CO<sub>2</sub>. At some pressures, when the CO<sub>2</sub> and oil are intimate contact, they will become miscible [26]. When the contact between oil and CO<sub>2</sub> occurs with little or no reservoir

mixing, the pressure at which miscibility happens is defined as the thermodynamic MMP. As shown in Figure 2.1, the purpose of miscible injection is to reduce the residual oil saturation by lowering the IFT between oil and the displacing fluid [10].

As shown in Figure 2.7, the displacement efficiency of CO<sub>2</sub> is plotted against the reservoir pressure. At pressure above MMP (higher than 1300 psig), the displacement efficiency exceed 90% and considered miscible. However, at pressure below MMP, the displacement efficiency decreases as the pressure reduced.

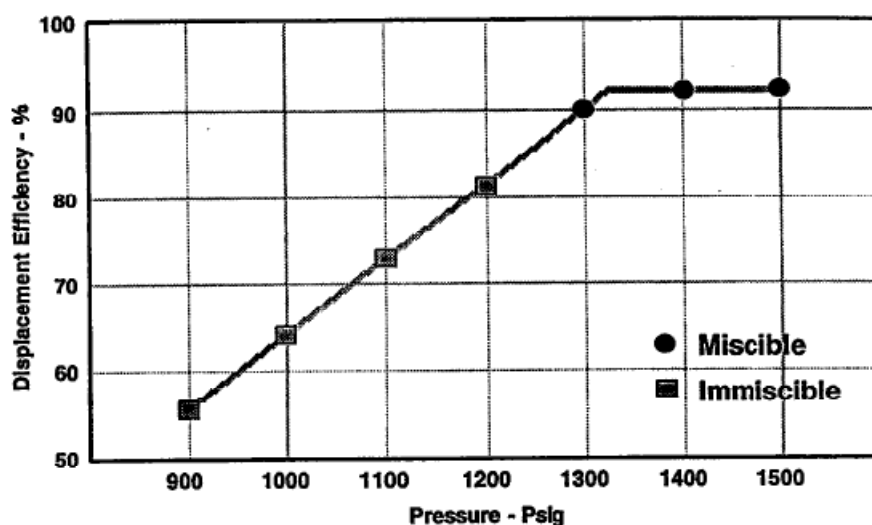


Figure 2.7 Slim tube miscibility test. [21]

## 2.5 CO<sub>2</sub> Fluid Properties

CO<sub>2</sub> is effective in improving oil recovery for two reasons: density and viscosity [26]. At high pressure, CO<sub>2</sub> forms a phase which density is close to that of a liquid, even though its viscosity remains quite low. Under miscibility condition in West Texas [26], the density of CO<sub>2</sub> typically is 0.7 to 0.8 g/cm<sup>3</sup>, not much less for oil and far above that of a gas such as methane, which is about 0.1 g/cm<sup>3</sup>. Dense-phase CO<sub>2</sub> has the ability to extract hydrocarbon than if it were in gaseous phase (and thus at lower pressure). The viscosity of CO<sub>2</sub> under miscible conditions in West Texas (0.05 to 0.08 cp) is significantly lower than that of fresh water (0.7 cp) or oil (1.0 to 3.0 cp).

For a constant temperature, CO<sub>2</sub> changes phase from gas to liquid as pressure increases, which cause dramatic changes in fluid properties like fluid density and viscosity. For example, by doubling pressure from 500 psia to 1000 psia, CO<sub>2</sub> density increases drastically 0.08 - 0.8 g/cm<sup>3</sup> as for its viscosity from 0.017 - 0.074 cp [26]. The CO<sub>2</sub> fluid properties are shown in Table 2.4 and Figure 2.8.

Table 2.4 Physical Properties of CO<sub>2</sub>. [46]

<i>CO<sub>2</sub> properties under Pressure 14.7 psig and Temperature 0 °C</i>	
Molecular Weight	44.01 g/mol
Specific Gravity	1.529
Density	1977 g/cm <sup>3</sup>
<i>Critical Properties</i>	
Temperature	31.05 °C
Pressure	1086 psig
Volume	94 cm <sup>3</sup> /mol
<i>Triple Point</i>	
Temperature	-56.6 °C
Pressure	89 psig

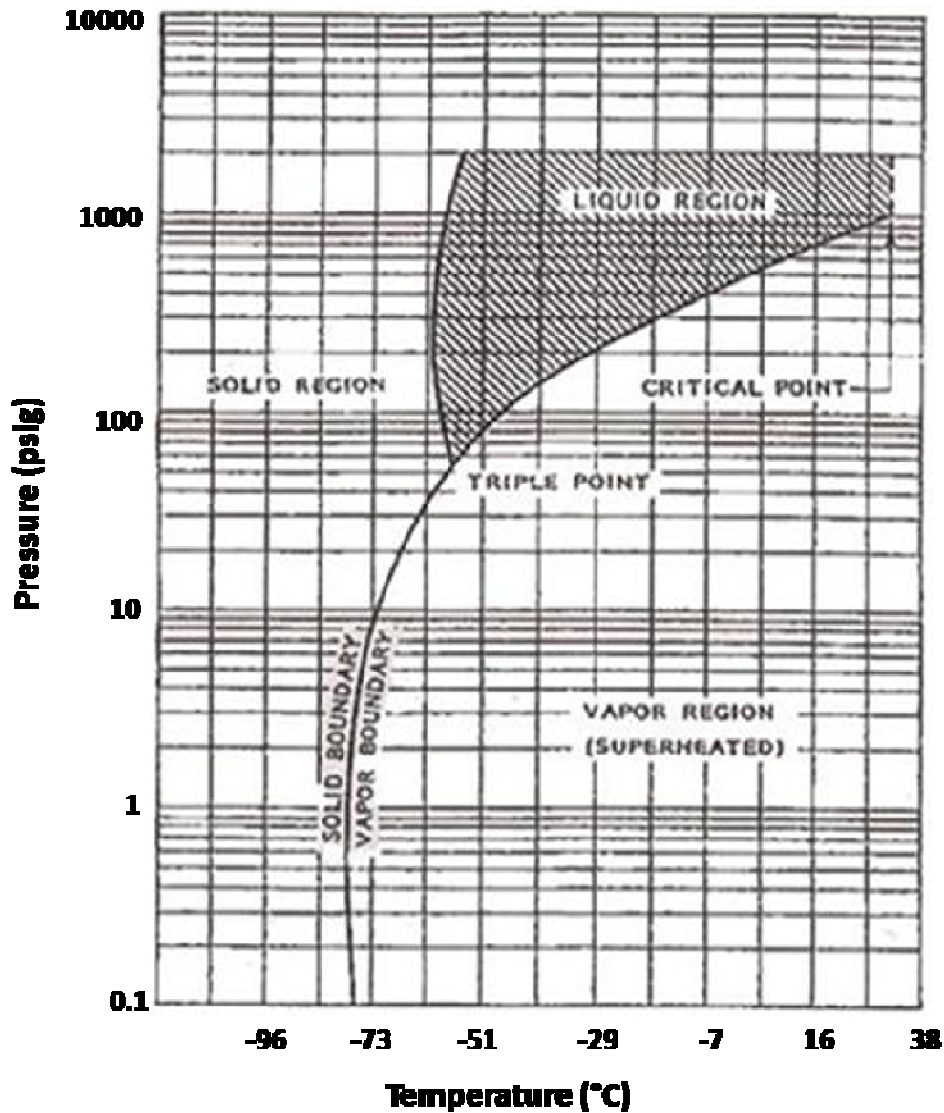


Figure 2.8 Phase Diagram of pure CO<sub>2</sub>. [26]

## 2.6 Mobility and Mobility Ratio

Mobility is defined as the ratio of the permeability to the viscosity. Meanwhile, mobility ratio is defined as the mobility of the displacing fluid divided by the mobility of the displaced fluid [10]. Mobility ratio is one of the most important parameters of a miscible displacement and has a great influence of volumetric sweep out of the solvent slugs.

Green and Willhite [47] explained that mobility of a fluid phase flowing in a porous medium is defined on the basis of Darcy equation:

$$u_i = - \left( \frac{k_i}{\mu_i} \right) \left( \frac{dp}{dx} \right) \dots\dots\dots (6)$$

where,

$u_i$  = Superficial (Darcy) velocity of phase  $i$ , D/ft<sup>2</sup>

$k_i$  = Effective permeability of phase  $i$ , md

$\mu_i$  = Viscosity of phase  $i$ , cp

$p$  = Pressure, psia

$x$  = Distance, ft

For single phase flow,  $k_i$  is the absolute permeability of porous medium. For multiphase flow, it is the effective permeability of flowing phase and a function of the saturation of the phase. Mobility of the fluid phase,  $\lambda_i$ , is given by:

$$\lambda_i = \left( \frac{k_i}{\mu_i} \right) \dots\dots\dots (7)$$

In calculations involving displacement process, mobility ratio ( $M$ ) can be calculated by using:

$$M = \frac{\lambda_D}{\lambda_d} \dots\dots\dots (8)$$

where,

$M$  = Mobility ratio, dimensionless

$\lambda_D$  = Mobility of the displacing fluid phase, md/cp

$\lambda_d$  = Mobility of the displaced fluid phase, md/cp

Consider in an idealized situation where solvent displaces oil at the irreducible water saturation and oil solvent mixing is negligible. No water is flowing and the

permeability to oil and solvent are equal. Mobility ratio in this case is simply the ratio of oil and solvent viscosities [10].

Green and Willhite [47] also explained that mobility ratio can be defined in a variety ways, depending on the flow conditions in a specific process. When one solvent is displacing a second solvent with which the first solvent is completely miscible and only one phase is flowing, Equation (8) can be rewritten as:

$$M = \frac{\mu_d}{\mu_D} \dots\dots\dots (9)$$

where,

$M$  = Mobility ratio, dimensionless

$\mu_d$  = Viscosity of the displaced fluid phase, md/cp

$\mu_D$  = Viscosity of the displacing fluid phase, md/cp

Mobility ratio affects both areal and vertical sweep, with sweep decreasing as the mobility ratio increases for given volume fluid injected. The flow become unstable or showing unfavorable mobility ratio when the value of  $M > 1$ . Conversely, a value of  $M < 1$  is a favorable mobility ratio [47] .

## 2.7 Previous Study of CO<sub>2</sub> Enhanced Oil Recovery

Brock and Bryan [15] exclusively reported the summary of historical CO<sub>2</sub> miscible floods as shown in Table 2.5.

Table 2.5 Summary of Selected CO<sub>2</sub> Miscible Flood Projects. [15]

Field	Lithology	Depth (ft)	Tr (°F)	φ (%)	k (md)	Net Pay (ft)	Oil Gravity (°API)	μ (cp)	Amount Injected (%HCPV)	Incremental Recovery (%OOIP)
<b>Field Scale</b>										
Dolarhide	Trip. Chert	7800	120	17.0	9.0	48	40	0.4	30	14.0
East Vacuum	Oolotic dol.	4400	101	11.7	11.0	71	38	1.0	30	8.0
Ford Geraldine	Sandstone	2680	83	23.0	64.0	23	40	1.4	30	17.0
Means	Dolomite	4400	100	9.0	20.0	54	29	6.0	55	7.1
North Cross	Trip. Chert	5400	106	22.0	5.0	60	44	0.4	40	22.0
Norhast Purdy	Sandstone	8200	148	13.0	44.0	40	35	1.5	30	7.5
Rangely	Sandstone	6500	160	15.0	5 to 50	110	32	1.6	30	7.5
SACROC (17 Pattern)	Carbonate	6400	130	9.4	3.0	139	41	0.4	30	7.5
SACROC (4 Pattern)	Carbonate	6400	130	9.4	3.0	139	41	0.4	30	9.8
South Welch	Dolomite	4850	92	12.8	13.9	132	34	2.3	25	7.6
Twofreds	Sandstone	4820	104	20.3	33.4	18	36	1.4	40	15.6
Wertz	Sandstone	6200	165	10.7	16.0	185	35	1.3	60	10.0
<b>Producing Pilots</b>										
Garber	Sandstone	1950	95	17.0	57.0	21	47	2.1	35	14.0
Little Creek	Sandstone	10400	248	23.4	75.0	30	39	0.4	160	21.0
Maljamar	Anhydrous dol.	4050	90	10.0	11.2	49	36	0.8	30	8.2
Maljamar	Dolomitic sand.	3700	90	11.0	13.9	23	36	0.8	30	17.7
North Coles levee	Sandstone	9200	235	15.0	9.0	136	36	0.5	63	15.0
Quarantine Bay	Sandstone	8180	183	26.4	230.0	15	32	0.9	19	20.0
Slaughter Estate	Dolomite	4985	105	12.0	8.0	75	32	2.0	26	20.0
Weeks Island	Sandstone	13000	225	26.0	1200.0	186	33	0.3	24	8.7
West Sussex	Sandstone	3000	104	19.5	28.5	22	39	1.4	30	12.9
<b>Nonproducing Pilots</b>										
Little Knife	Sucr. Dolomite	9800	245	21.0	30.0	16	41	0.2	22	8.0
South Pine	Cryst. Dolomite	9000	205	17.0	10.0	11	32	1.8	-	-

The CO<sub>2</sub> miscible flood projects were divided into three categories: field scale, producing pilots, and non producing pilots. Field scale projects involved multiple patterns and were typically commercial projects. Producing pilots were pilot floods that used a producing well, while non producing pilots were pilot floods with observation wells only.

Frailey et.al. [48] published a research plan to study the use of depleting oil reservoirs with  $T_f$  less than  $T_{cCO_2}$  to sequester and investigate the implications of EOR from the liquid CO<sub>2</sub> displacement processes. They found that most of all depleting Low Temperature Oil Reservoir (LTOR) provide a unique opportunity for liquid CO<sub>2</sub> storage and its application as EOR method. Recent calculations indicate that oil remaining resources in the Illinois Basin may be as much as 5.9 billion barrels with produced oil only 450 million barrels. Data showed that the regional rule of thumb temperature gradient of Illinois Basin is 1 °F/100 ft and annual average temperature of 62°F at 100 ft below surface based on 40 years observation. For example, 70°F correspond to 900 ft and 88°F corresponds to 2700 ft. Based on these findings, it was

concluded that the range of formation depths for liquid CO<sub>2</sub> flooding can be identified at the selected places as shown in Figure 2.9. To one side, liquid CO<sub>2</sub> should be applicable in other basins e.g. the Appalachian and Arkoma Basin.

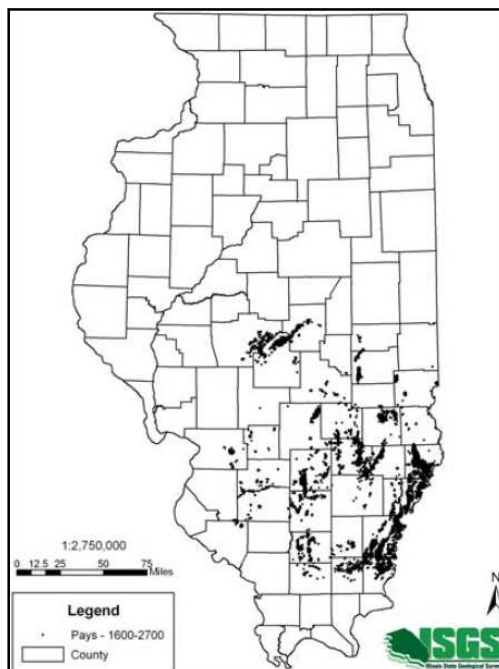


Figure 2.9 Oil fields producing from formations with  $T_f$  less than  $T_{cCO_2}$  and initial pressure greater than the saturation pressure of CO<sub>2</sub> at that formations temperature. [48]

Al-Quraini [49] conducted simulation study of water and CO<sub>2</sub> injection strategies in heavy oil West Sak Reservoir, North Slope Alaska. At the depth that hydrocarbon reservoirs are usually found, the reservoir temperature is usually above CO<sub>2</sub> critical temperature, resulting in gaseous neither supercritical state. However, Permafrost (soil at or below the freezing point of water), overlaying most of this field resulting the average reservoir temperature range between 50 °F and 100 °F. The study concluded that by injecting 0.91 PV of CO<sub>2</sub> at the rate of 150 b/d could produce 34.5 % of the OOIP. Al-Quraini concluded that in West Sak heavy oil reservoir, continuous liquid CO<sub>2</sub> injection produced almost the same amount of oil compared to water flood as a result of low mobility of liquid CO<sub>2</sub> compared to CO<sub>2</sub> gas.

Lindeberg and Holtz [50] experimented and perform simulation study as the validation of miscible CO<sub>2</sub> injection in the North Sea. The laboratory experiment was conducted by using 60 cm long and 3.8 cm diameter of Bentheimer sandstone with injection pressure of 310 bar and temperature of 116 °C. This study concluded that CO<sub>2</sub> injection successfully escalated the cumulative oil production up to 62.5% of OOIP after 25 years injection of 0.75 PV of CO<sub>2</sub>. Regarding pressure variation during the experiment and simulation, it indicates that higher pressure in the flooding operation enhances miscibility and flood stabilization caused by lesser density difference in the gravity established flood.

Beeson and Ortloff [51] published a study about investigation of water-driven carbon dioxide bank to recover crude oil. The experimental studies dealt with both high viscosity and low viscosity crude oil. The Ada crude oil with viscosity of 400 cp was displaced from 10 ft Torpedo sandstone model. Then again, Loudon crude oil with viscosity of 6 cp was displaced from 16 ft Weiler sandstone. On Ada crude oil experiment, the oil recovery equal to 52% after injecting 1.48 PV of liquid CO<sub>2</sub>. Meanwhile, 50 % of oil recovery was gained on Loudon crude oil after injecting water followed by 0.2 PV CO<sub>2</sub> bank.

## CHAPTER 3

### RESEARCH METHODOLOGY

This research was initiated by IFT measurement between the crude oil and CO<sub>2</sub> at various equilibrium pressures. The MMP of core flood condition was then estimated by the combination of Lasater and Holm Josendal correlation. Finally, the core flood laboratory experiment was conducted to study the effects of liquid CO<sub>2</sub> for enhancing oil recovery. The flowchart diagram of this research is shown in Figure 3.1.

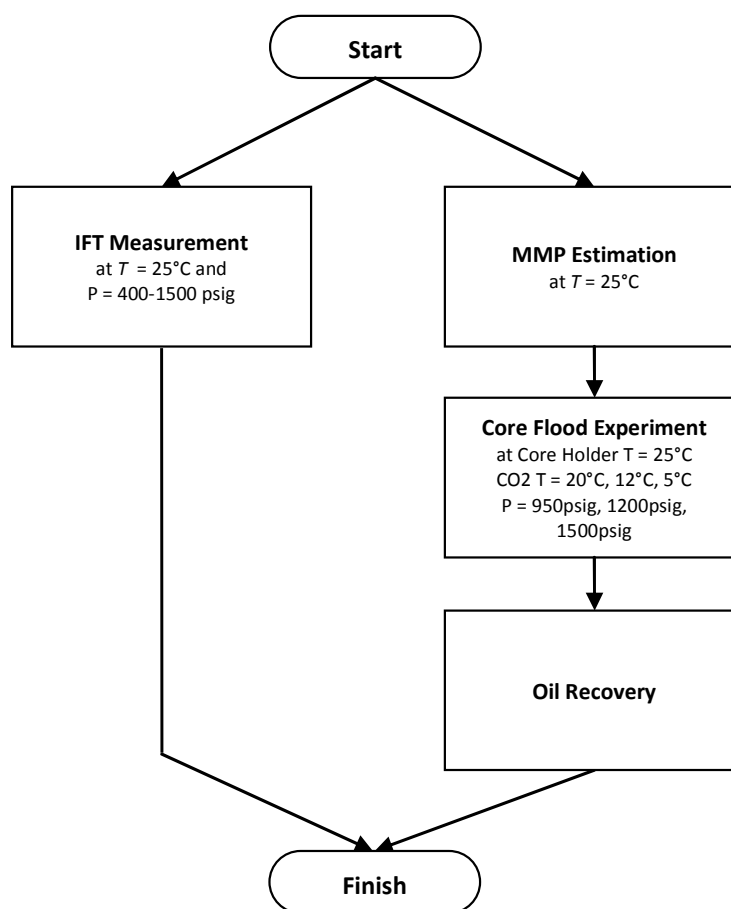


Figure 3.1 Research methodology flowchart diagram.

### 3.1 CO<sub>2</sub>-Crude Oil IFT Measurement

Interfacial Tension measurement between crude oil and CO<sub>2</sub> in this study is conducted experimentally by using IFT-700. This equipment consists of Smart Software interface, camera, positive displacement pump, and high pressure chamber and accumulator. The pendant drop method is used in this experiment because the density of crude oil is lower than the density of CO<sub>2</sub> during all experiment condition.

#### 3.1.1 Flowchart Diagram of IFT Measurement

The flowchart diagram of IFT measurement carried out in this is study shown in Figure 3.2 and the procedures is given in Appendix A.

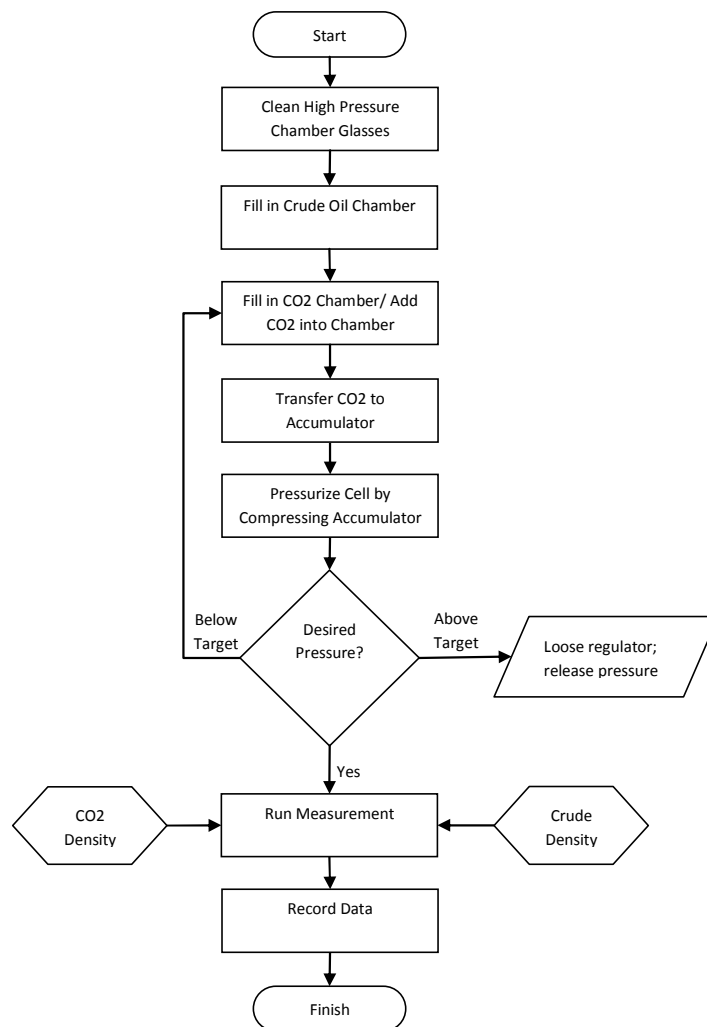


Figure 3.2 Flow Diagram of IFT measurement.

### 3.1.2 IFT Measurement Apparatus

Various IFT measurement techniques have been reported in literatures during the last century [32] [33] [34] [35]. One of the techniques is called pendant drop method. Pendant drop case is used to measure the static equilibrium interfacial tensions of crude oil-CO<sub>2</sub> system at different equilibrium pressures and constant temperature. In this study, the same technique was applied to determine the IFT between the CO<sub>2</sub> and crude oil. The equipment IFT-700 manufactured by Vinci Technologies can provide the pendant drop method for IFT measurement. A schematic diagram for IFT-700 that is used in this study is shown in Figure 3.3.

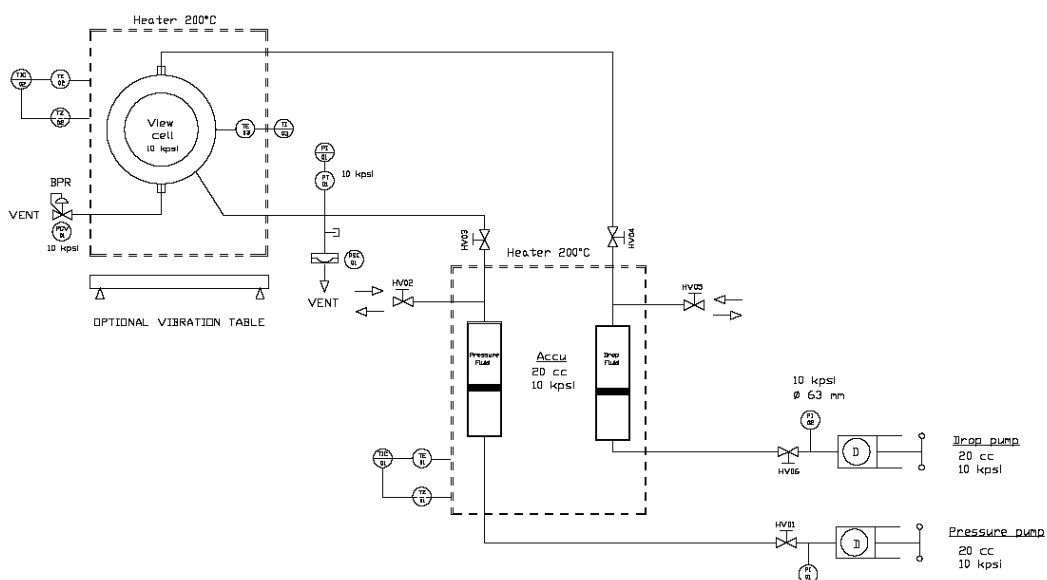


Figure 3.3 Schematic Diagram of IFT-700.

The main component of IFT-700 in this experimental set-up is a see-through windowed high-pressure cell. The maximum operating pressure and temperature of this pressure cell are equal to 10,000 psig and 200°C, respectively. Pendant drop is chosen due to higher density value of crude oil compared to CO<sub>2</sub> at the respected condition. The equilibrium pressure inside the pressure cell is measured by using a digital pressure gauge.

A light source and a glass diffuser were used to provide uniform illumination for the pendant oil drop. A microscope camera is used to capture the digital images of the pendant oil drop inside the pressure cell at different times. The high pressure cell is positioned horizontally between the light source and the microscope camera. These equipments are placed on a vibration free table as shown on Figure 3.4.



Figure 3.4 A Camera and High Pressure Cell on IFT-700.

### 3.2 MMP Estimation

MMP estimation in this study is carried out by using the combination method of Lasater and Holm-Josendal. The procedures are listed as below:

1. Crude oil specific gravity at standard condition is determined by using Equation (4).

$$\gamma = \frac{\rho_o}{\rho_w} \dots\dots\dots (4)$$

2. Oil API degree of crude oil is determined by using Equation (5).

$$^{\circ}API = \frac{141.5}{\gamma} - 131.5 \dots\dots\dots (5)$$

- The C<sub>5+</sub> effective molecular weight of crude oil is determined by using Equation (3).

$$MW = \left( \frac{7864.9}{^{\circ}API} \right)^{\frac{1}{1.0386}} \dots\dots\dots(10)$$

- MMP of crude oil and CO<sub>2</sub> by is determined by using Equation (2), at the respected temperature.

$$MMP = -329.558 + (7.727 * MW * 1.005^T) - (4.377 * MW) \dots\dots\dots(11)$$

### 3.3 Core Flood Test

The core flood experiment carried out in this study was conducted in laboratory by means of core displacement equipment which consists of two units of parallel positive displacements pumps and three units of high pressure accumulator to collect the injection fluid before displacement.

#### 3.3.1 Flowchart Diagram of Core Flood Test

The flowchart diagram of core flood experiment carried out in this is study shown in Figure 3.5 and the detail procedure is shown in Appendix B.

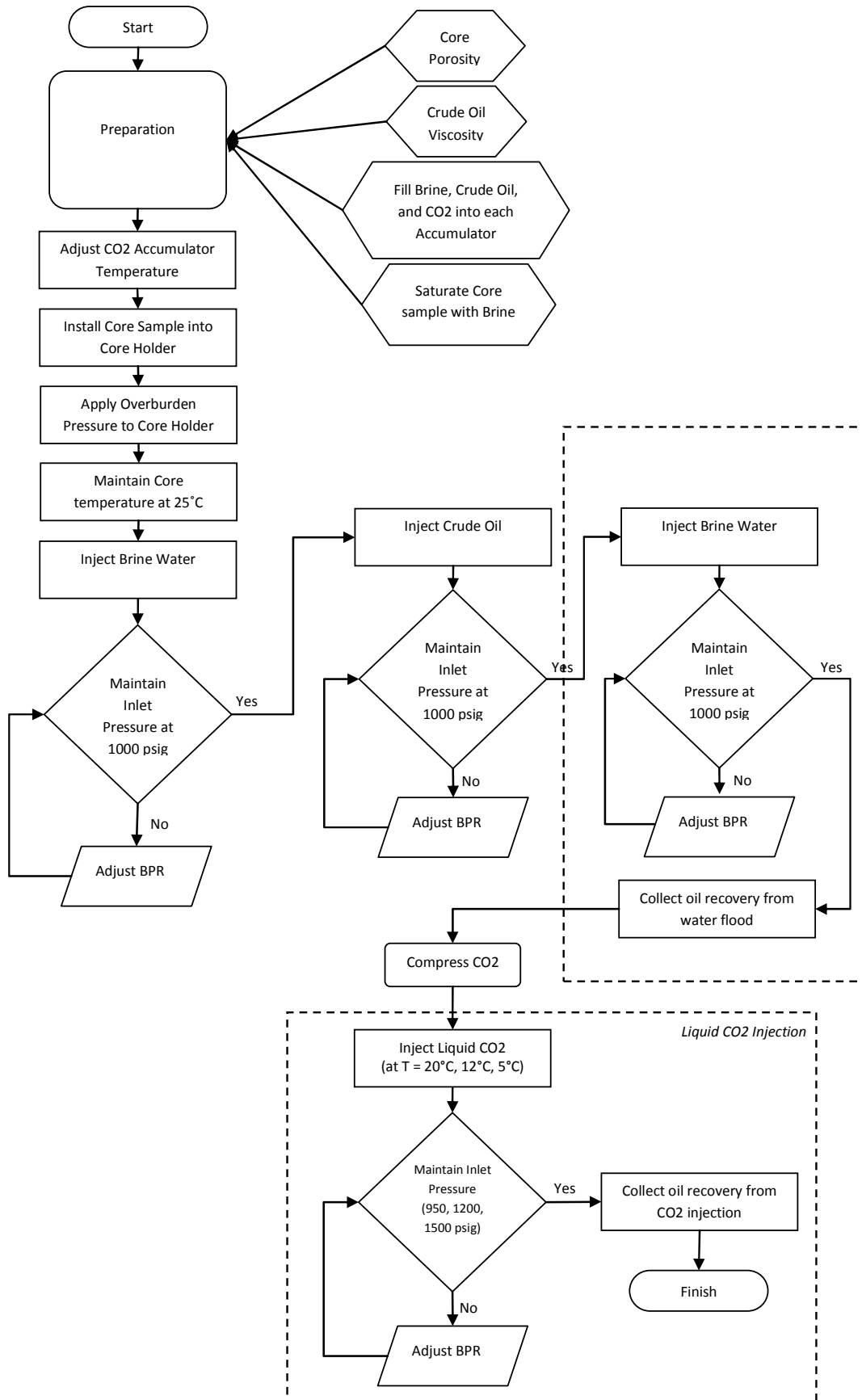


Figure 3.5 Flow Diagram of CO<sub>2</sub> Core Flooding Experiment.

### 3.3.2 Porosity Measurement

The equipment that is used to measure the porosity of core sample in this study is PoroPerm manufactured by Vinci Technologies. Two types of gases are required to operate this equipment, first is Nitrogen as the confining pressure conditioning and valve operation, and second is Helium as porosity measurement purpose. The core sample porosity measurement procedure carried out in this study is given in Appendix C.

PoroPerm is completed with computer operated software which helpful in operation and data recording. The measurement is based on the unsteady state method (pressure fall off) whereas the pore volume is determined using Boyle's law technique. This equipment has been calibrated previously before the measurement was conducted.

For measurement is simply by installing the core into the core holder and run the calculation in the software interface. The equipment is shown in Figure 3.6.



Figure 3.6 PoroPerm equipment to measure core porosity.

### 3.3.3 Density Measurement

The density of liquid that is used in this study is measured by using Anton Paar DMA 35N Portable Density Meter. Anton Paar Portable Density Meter contains density

reading and the respected temperature of measurement. The equipment working procedure is to draw the fluid into the chamber inside it and measure the density on the respected temperature as explained in Appendix D.

Before utilizing this equipment, a calibration step was conducted by measuring the density of distilled water at temperature of  $T = 26.8^{\circ}\text{C}$ . The measured density of distilled water at this condition was  $0.998 \text{ g/cm}^3$ . There is an error of 0.1% compared with the density value of 0.997 taken from the density table published by Perry [52]. This error value can be considered as negligible due to its very small value and the equipment is accurate for density measurement.

Density and temperature value is displayed in  $\text{g/cm}^3$  and degree Celsius. The portable density meter utilized is shown in Figure 3.7.



Figure 3.7 Portable Density Meter equipment to measure liquid density.

### 3.3.4 Initial Core Saturation

Manual Saturator is used for initial saturation of the core sample with brine water. Load the clean and dry core sample into the Manual saturator and set the pressure condition inside the chamber to 1,200 psig. Core saturation requires at least 8 hours at the equilibrium pressure condition. The picture of Manual Saturator is shown in Figure 3.8 and the procedure carried out in this study is given in Appendix E.



Figure 3.8 Manual Saturator for core sample initial saturation.

### 3.3.5 Core Flood Test Apparatus

The core flood equipment used in this experiment is Temco RPS-830-10000 HTHP Relative Permeability Test System. This advance equipment has the capacity to measure the effective permeability of liquid-liquid and liquid-gas. The system is provided with Smart Series Software™ for data acquisition, control and report writing. The software interface is as shown by Figure 3.9.

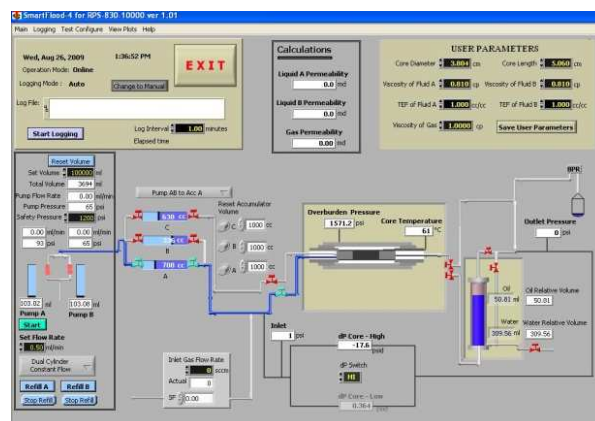


Figure 3.9 Smart Series Software™ Interface on RPS-830 Relative Permeability Test Equipment.

The equipment consists of three separated accumulator to gather each of injection fluids which could endure up to 10,000 psig and temperature 220°C. Since the tests in this study require low temperature conditioning, an additional water bath is installed to level down the temperature of CO<sub>2</sub>, as shown in Figure 3.10 and Figure 3.11. The water bath is placed in the equipment to sink CO<sub>2</sub> accumulator exclusively for leveling down its temperature to the desired condition. The image of Experiment Schematic Diagram, Water Bath, and RPS Control Panel is shown by Figure 3.10, Figure 3.11, and Figure 3.12.

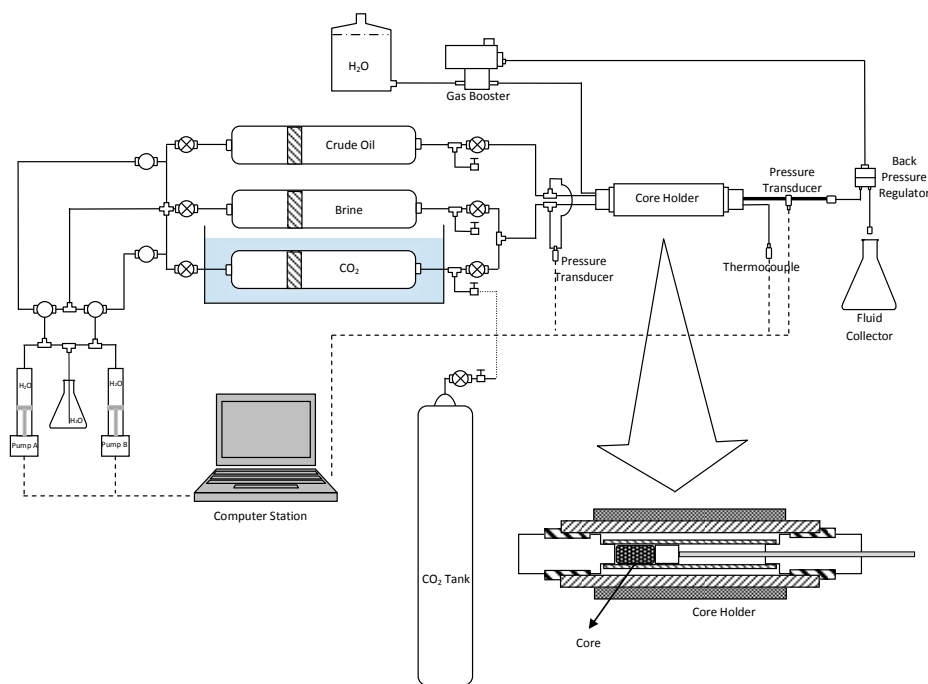


Figure 3.10 Schematic diagram of the experimental set-up for Core Flooding.



Figure 3.11 Water Bath for CO<sub>2</sub> temperature conditioning.



Figure 3.12 Panels to operate RPS-830.

### 3.3.6 Core Sample Cleaning

The core cleaning process in this study is using Soxlet Extractor. The principal of this equipment is to clean any fluids remaining within the pore space by introducing vaporized cleaning agent into the core sample. The cleaning agent that is used in this process is Toluene because of its ability to dissolve the residual crude oil in the core sample and flush it out of the core sample. The cleaning process requires at least 3 days to ensure the core sample is cleaned from any residual oil. The equipment is shown in Figure 3.13.



Figure 3.13 Soxhlet Extractor for core cleaning by using Toluene as Cleaning Agent.

The summary of the core flooding procedure in this study is shown in Table 3.1 below.

Table 3.1 Summary of injection procedures for core flood tests.

Procedure	Injection Volume		Injection Rate, ml/min	Injection Time, hour
	ml	PV		
Initial Brine Saturation	100	6.4	3	0.56
Crude Saturation	200	12.8	0.8	4.17
Water Flood	150	9	3	0.83
Liquid CO <sub>2</sub> Injection	163	10	1	2.72

## CHAPTER 4

### RESULTS AND DISCUSSIONS

#### 4.1 MMP Estimation by Using the Combination of Lasater and Holm-Josendal Correlation

There are several factors affecting MMP. Some of these factors are oil properties, reservoir temperature, reservoir pressure, and the purity of the injected CO<sub>2</sub> [26]. This study also give an account of MMP estimation of CO<sub>2</sub> flooding by using the combination of Lasater [45] and Holm-Josendal [42] which was empirically correlated by Holtz et.al. [40]. MMP estimation with this method was based on reservoir temperature and oil properties data (effective molecular weight of C<sub>5+</sub> component exclusively).

As published in literatures [32] [33] [34], the IFT between two immiscible fluid decreases as the pressure increases, until finally approaching zero. When the IFT is approaching zero, both of these fluids are completely miscible [10] [26]. In the previous chapter of this thesis, Figure 2.1 showed the effect of IFT between solvent and crude oil in terms of capillary number to the residual oil saturation for displacement process. Here, the residual oil saturation is plotted against the capillary number, the product of Darcy Velocity and oil viscosity divided by IFT. This figure shows that a drastic reduction of IFT between crude oil and solvent is required to achieve a significant reduction in enhance oil recovery.

Therefore, the purpose of estimating MMP in this study was to generate a miscible displacement during the core flood experiment to achieve significant reduction in residual oil saturation.

A two-step approach had been taken to estimate the MMP. First, the molecular weight of  $C_{5+}$  components of the reservoir oil must be determined by using a correlation between oil API gravity and  $C_{5+}$  effective molecular weight which was published by Lasater [45]. The measured density of crude oil sample and water at 15.6°C (equal to 60°F) was 0.82 gr/cm<sup>3</sup> and 0.998 gr/cm<sup>3</sup> respectively. With these results, the calculated specific gravity of crude oil sample 0.822 consequently, by using Equation (4). Afterward, oil API degree of crude oil sample was determined by using Equation (5) which resulted 40.7 °API respectively. Finally, the effective molecular weight of  $C_{5+}$  was calculated by using Equation (3). The value of effective molecular weight of  $C_{5+}$  from this calculation was 158.8 lb mol.

Second, the MMP was calculated by using Holm-Josendal [42] correlation which was represented by Equation (2). At temperature 25°C (equal to 77 °F), core flood temperature of this experiment, and effective molecular weight 158.8 lb mol, the value of MMP estimated was 671 psia. The calculations step carried out for MMP estimation in this study is shown in Appendix F.

The result of estimated MMP calculation steps is summarized in Table 4.1.

Table 4.1 Calculation summary of estimating MMP.

Parameter	Calculation Result	Unit
$\gamma$	0.822	(dimensionless)
°API	40.7	° API
<i>MW</i>	158.8	lb mol
<i>MMP</i>	671	psia

The MMP condition falls under the vapor phase when projected into Figure 2.8. According to this estimation, every displacement pressure higher than 671 psia at  $T = 25^\circ\text{C}$  results in miscible displacement between crude oil and CO<sub>2</sub> injected with this crude oil sample. There are two boundary conditions required to fulfill miscibility in this estimation. First, the displacement pressure should be above the MMP to attain miscibility. Second, the injection pressures and temperatures should be within the

liquid phase area if projected into Figure 2.8. Thus, it is acceptable whether the MMP estimated by this method is within the vapor area as long as the displacement condition is in liquid CO<sub>2</sub> phase region.

## 4.2 Effect of CO<sub>2</sub> injection to Oil Recovery on Core Flood Tests

### 4.2.1 Porosity Measurement Results

Three Berea Sandstone core samples were used in this study with diameter of 1.5 inch and length of 3 inch. The porosity measurement results for each core sample are shown in Table 4.2.

Table 4.2 Porosity measurement results of Berea Sandstone by using PoroPerm.

Core No.	$V_p$ (ml)	$V_g$ (ml)	$V_b$ (ml)	$\phi$ (%)
1	15.76	71.11	86.87	18.14
2	16.83	70.04	86.87	19.38
3	15.38	71.49	86.87	17.70

The porosity difference of all cores in this study was not significant with value of 18.14%, 19.38% and 17.70%. The same value of porosity was also produced after measurement on opposite flow direction of the core plug by using PoroPerm Equipment.

### 4.2.2 Core Flood Experiment Results

The complete experiment results of core flood tests are shown in Table 4.3 and Figure 4.1 and the calculation procedure is shown in Appendix.

Table 4.3 Core flood injection profile and oil recovery.

Exp. No.	Inlet Pressure (psig)	CO <sub>2</sub> Temp. (°C)	Core No.	$\phi$ (%)	OOIP (%PV)	Water Injected (PV)	Water Flood Oil Recovery (% OOIP)	Sorw (%PV)	Vol. CO <sub>2</sub> Injected (PV)	CO <sub>2</sub> Oil Recovery (%OOIP)
1	950	5	2	19.4	90.9	8.9	37.9	62.1	10	33.7
2	950	12	2	19.4	89.7	8.9	39.7	60.3	10	26.4
3	950	20	2	19.4	90.3	8.9	38.8	61.2	10	24.7
4	1200	5	3	17.7	96.9	9.8	37.6	62.4	10	54.8
5	1200	12	1	18.1	98.4	9.5	36.1	63.9	10	47.5
6	1200	20	1	18.1	98.4	9.5	35.5	64.5	10	43.0
7	1500	5	2	19.4	89.7	8.9	37.7	62.3	10	73.4
8	1500	12	3	17.7	97.6	9.8	37.3	62.7	10	71.3
9	1500	20	1	18.1	95.2	9.5	38.0	62.0	10	67.7

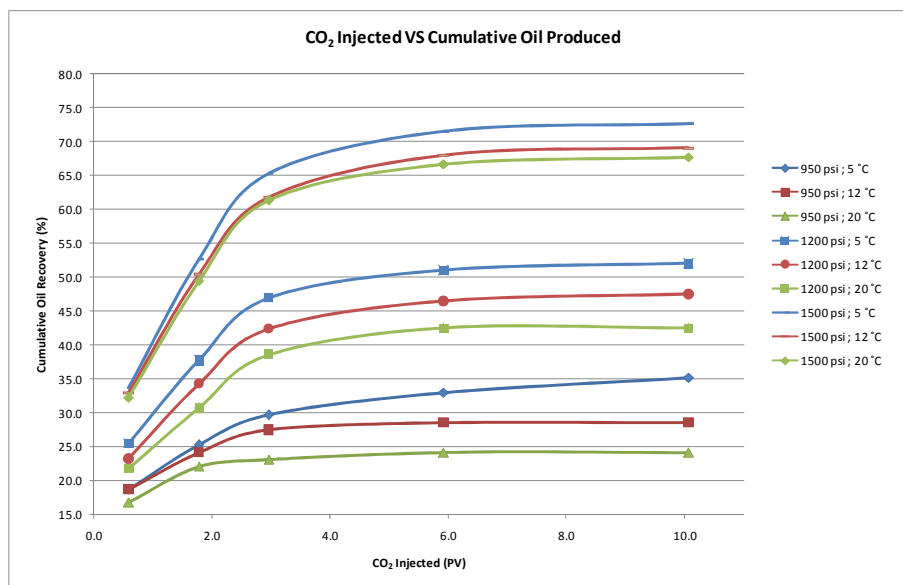


Figure 4.1 Oil recovery as effect of liquid CO<sub>2</sub> injection at various pressures and temperatures of CO<sub>2</sub> injected.

In these experiments, the crude oil was injected to saturate the core initially. The injection flow rate applied was 0.8 ml/min for at least 4 hours to displace 200 ml of crude oil. Higher injection flow rate would cause significant pressure difference in the porous medium due to viscosity effect of crude oil. As effect of this process, the outcome of original oil in place was such limits from 89.7 % to 98.4 % of pore volume and leaving the value of initial water saturation below 11%. This phenomenon

happened due to the capillary end effect. Peters [53] explained that during displacement if a medium is flooded with the wetting phase (brine) initially, only the non-wetting phase will be expelled from the outlet end at higher capillary pressure than outside. When the wetting phase arrives at the outlet end, the system now has the chance to seek capillary equilibrium which will be achieved by the accumulation of the wetting phase at the outlet end. An experiment conducted by Perkins [54] also proven the occurrence of this phenomenon where the capillary end effect was significantly reduced at high injection pressure.

All water floods were conducted at flow rate 3 ml/min and total volume water injected 150 ml. Experiment 1, 2, 3 and 7 were using the same core sample in core flood experiment. Although the same water flood action performed to these cores, as shown in Table 4.3, oil recovery from water flood was ranging in such limits from 36.1 % until 39.7 %. The same condition happened on experiment 5, 6 and 9 which recover 36.1 %, 35.5 %, and 38 % of original oil in place. As for experiment 4 and 8, oil recovery by water flood was 37.6 % and 37.3 % of the original oil in place.

It was observed that oil recovery to CO<sub>2</sub> injection on experiment 1, 2, and 3 increases with the decreasing temperature of CO<sub>2</sub> injected. High recovery of crude oil was produced during early CO<sub>2</sub> injection until 3 PV as shown in Figure 4.2 until Figure 4.4. This was attributed to the improved mobility ratio at liquid region of CO<sub>2</sub> injected which gives better sweep efficiency. Lower temperature at constant pressure results in higher viscosity of CO<sub>2</sub>. This condition would help in increasing the displacement sweep efficiency and prevent or at least reduce the occurrence of fingering phenomena. High viscosity of displacing agent would reduce bypassing phenomena that commonly happens in continuous gas CO<sub>2</sub> flooding [48]. The same occurrence appeared in experiment 4, 5, 6 as well as in experiment 7, 8, 9, where the oil recovery increasing as the temperature CO<sub>2</sub> injected decreases if the pressure remains constant.

High recovery of crude oil was produced during early CO<sub>2</sub> injection until 3 PV. From this point further, injection of liquid CO<sub>2</sub> produced a lesser amount of crude oil than 5% of originally oil in place. This is because the residual oil saturation by injecting the liquid CO<sub>2</sub> had been reached. The viscous force of liquid CO<sub>2</sub> injected had been smaller to the capillary force and not able to sweep the remaining oil in porous

medium. The velocity of liquid within the swept region tends to be higher compared to the unswept region. Therefore, if most of the crude oil had been removed from the pore space, the pore that is left behind tends to easily passed by the following liquid CO<sub>2</sub> due to no resistance by the crude oil anymore.

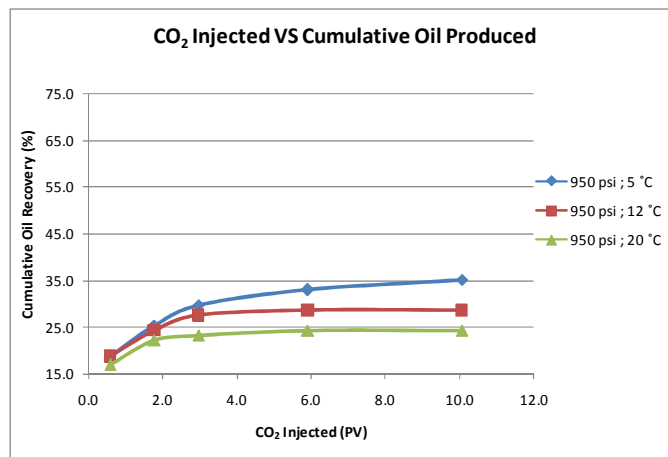


Figure 4.2 Oil recovery as effect of CO<sub>2</sub> injection at 950 psig.

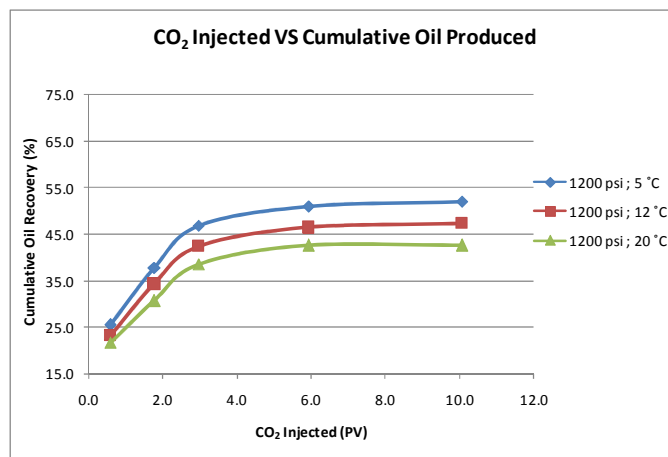


Figure 4.3 Oil recovery as effect of CO<sub>2</sub> injection at 1200 psig.

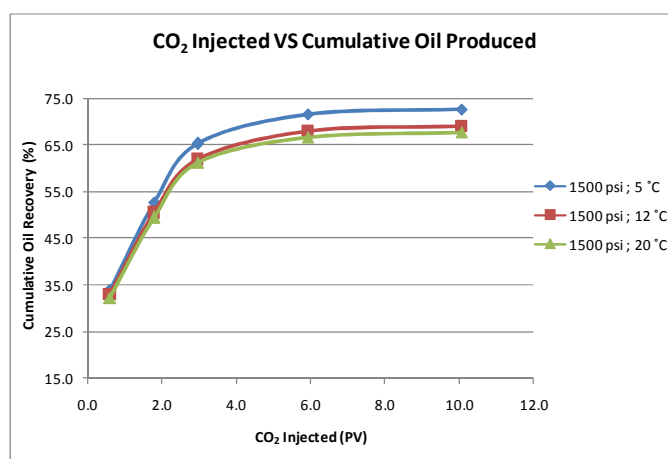


Figure 4.4 Oil recovery as effect of CO<sub>2</sub> injection at 1500 psig.

In Figure 4.1, the oil recovery was low at injection pressure of 950 psig although literature [26] showed that under this circumstance the CO<sub>2</sub> was in liquid phase. However, the CO<sub>2</sub> phase changes to gas at 933 psig at temperature of  $T = 25^{\circ}\text{C}$ . From this threshold condition, slight reduction of pressure below 950 psig could vaporize the liquid CO<sub>2</sub> to gas phase. During core flood experiment, the experiment was conducted at constant flow rate injection at all time. The purpose of this step was to maintain the displacement front velocity during core flooding remain constant while injecting at constant pressure. Thus, in order to maintain the inlet pressure at the desired value, the back pressure valve must be adjusted manually trough all experiment. If this condition was not fulfilled, the displacement process would have been completed in shorter time and the miscibility would not have been attained completely due to short time interaction between CO<sub>2</sub> and crude oil. It was recorded that during the CO<sub>2</sub> injection, the pressure difference between inlet and outlet of core holder was in range of 37-93 psig. The small pressure difference could transform portion of the liquid CO<sub>2</sub> to its gas state and immediately breakthrough to the outlet end and bypass the remaining oil in the core sample.

As the CO<sub>2</sub> injection pressure increased (i.e. 1200 psig and 1500 psig), the oil recovery was significantly increased. The increased oil recovery by escalating injection pressure was due to the increased viscosity and density of the injected CO<sub>2</sub> [48] [49]. High injection pressure also acted during this condition which displacing oil with better performance.

Experiment 1, 4, and 7, shows variation in oil recovery with value 24.7%, 43%, and 67.7% respectively. This comparison is based on constant temperature at different injection pressures. It was found that the effect of escalating injection pressure gives higher recovery compared to reducing temperature of CO<sub>2</sub> injected [48] [49] as shown in Figure 4.5 and Figure 4.6.

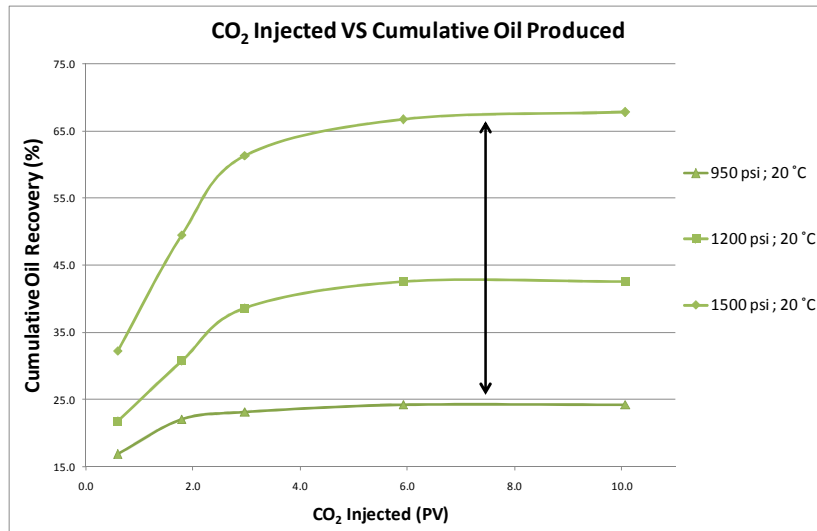


Figure 4.5 Oil recovery at constant CO<sub>2</sub> temperature of  $T = 20^{\circ}\text{C}$  and various injection pressure.

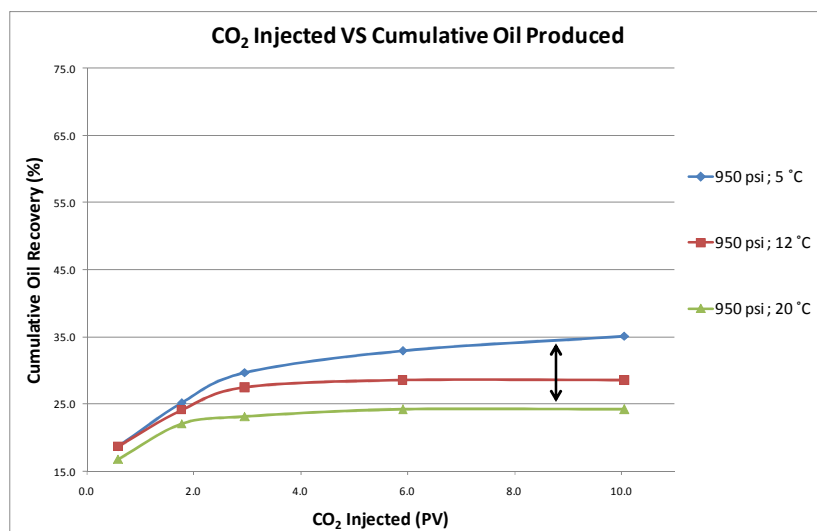


Figure 4.6 Oil recovery at constant injection pressure of  $P = 950$  psig and various injected CO<sub>2</sub> temperature.

The same condition happens for other conditions as shown in Figure 4.7 until Figure 4.10.

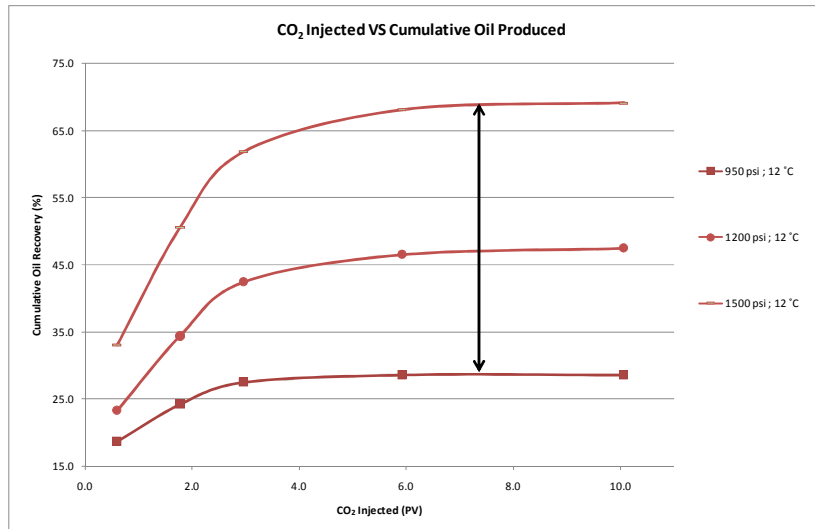


Figure 4.7 Oil recovery at constant CO<sub>2</sub> temperature of  $T = 12^{\circ}\text{C}$  and various injection pressure.

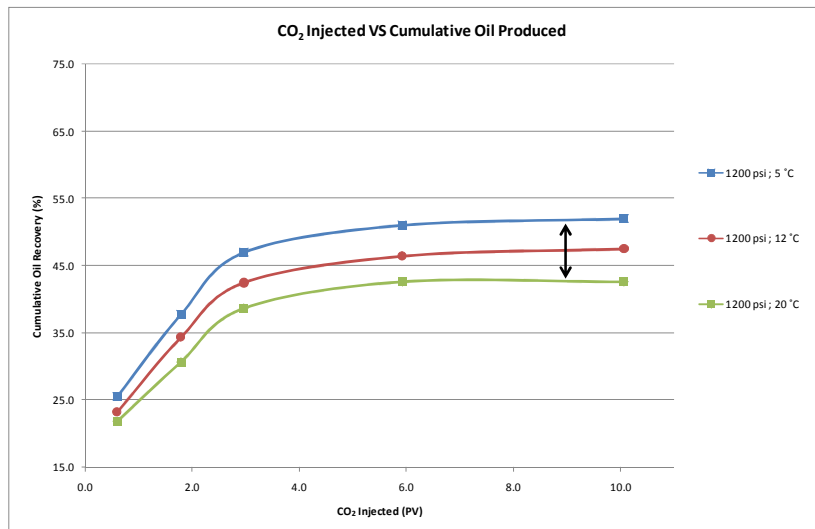


Figure 4.8 Oil recovery at constant injection pressure of  $P = 1200$  psig and various injected CO<sub>2</sub> temperature.

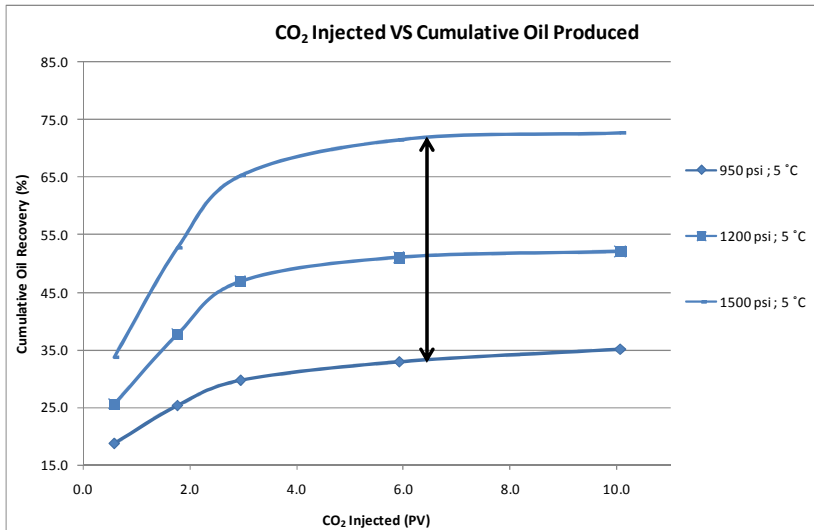


Figure 4.9 Oil recovery at constant CO<sub>2</sub> temperature of  $T = 5^{\circ}\text{C}$  and various injection pressure.

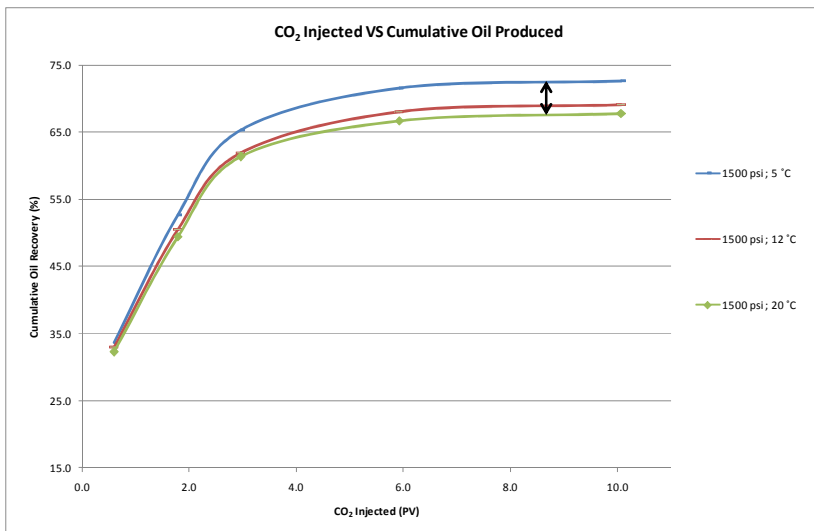


Figure 4.10 Oil recovery at constant injection pressure of  $P = 1500$  psig and various injected CO<sub>2</sub> temperature.

All tests in this study shows that high oil recovery yielded since early production until 3 PV of CO<sub>2</sub> injected. Injecting more CO<sub>2</sub> above this value only caused small effect to oil recovery and ineffective in economic sense. This is due to the fact that after CO<sub>2</sub> breakthrough, the injected CO<sub>2</sub> bypassed and failed to effectively displace the crude oil inside the core. In this case, the oil production is significantly reduced whereas the solvent production increases.

Subcritical solubility of CO<sub>2</sub>-crude oil and liquid condensation mechanisms are expected to reduce CO<sub>2</sub> gas bypassing. Table 4.4 shows the value of liquid CO<sub>2</sub> viscosity range in this experiment. The average value on Table 4.3 shows that liquid CO<sub>2</sub> viscosity approximately 6 – 8 times higher to its gas state. At saturation pressure, CO<sub>2</sub> gas starting to change phase and a portion begins to condense. CO<sub>2</sub> liquid condensation results in a viscosity increase, which reduces the mobility of the CO<sub>2</sub>, and thereby reduces bypassing. The decrease of oil viscosity due to CO<sub>2</sub> solubility and the high viscosity of CO<sub>2</sub> (compared to gaseous phase), reduces its mobility and increase the CO<sub>2</sub>-crude oil contact period.

### 4.2.3 Mobility Ratio Calculations

The viscosity data of various conditions in this experiment is displayed in Table 4.4. By applying the formula in Equation (9) into the available viscosity data in Table 4.4 and measured viscosity of crude oil sample is 2.33 cp at  $T = 25\text{ }^{\circ}\text{C}$ , mobility ratio calculation results is shown in Table 4.5.

Table 4.4 CO<sub>2</sub> Viscosity properties at several pressures and temperatures in this study.  
(after Jarrel et.al [26])

Pressure (psig)	CO <sub>2</sub> Viscosity at Temperature (centipoises)				
	25°C	20°C	12°C	5°C	
400	0.0162	0.0160	0.0158	0.0157	} Gas
500	0.0167	0.0166	0.0165	0.0163	
600	0.0172	0.0172	0.0174	0.0965	} Liquid
700	0.018	0.0181	0.0831	0.0990	
800	0.0189	0.0169	0.0893	0.1009	
950	0.0713	0.0770	0.0920	0.1035	
1100	0.0722	0.0812	0.0949	0.1060	
1200	0.0752	0.0834	0.0966	0.1075	
1500	0.0818	0.0890	0.1014	0.1119	

Table 4.5 Mobility Ratio calculation results at liquid CO<sub>2</sub> condition.

Pressure (psig)	Mobility Ratio at injection temperature				
	25°C	20°C	12°C	5°C	
400	143.8	145.3	147.4	148.3	} Gas
500	139.5	140.6	141.3	142.5	
600	135.5	135.1	133.6	24.2	} Liquid
700	129.4	128.4	28.0	23.5	
800	123.3	138.2	26.1	23.1	
950	32.7	30.2	25.3	22.5	
1100	32.3	28.7	24.6	22.0	
1200	31.0	27.9	24.1	21.7	
1500	28.5	26.2	23.0	20.8	

As mentioned by Green and Willhite [47], that during miscibility displacement, the mobility ratio of displaced fluid and the displacing fluid is equal to the ratio of its viscosity in that condition. Assuming that the residual water saturation prior to liquid CO<sub>2</sub> injection was approaching zero, this estimation is considered to be valid between two existing fluid (liquid CO<sub>2</sub> and crude oil).

The calculations in Table 4.5 showed that the mobility ratio in this study varies in value 32.7, 31, and 28.5 depend on the inlet pressure and  $T = 25^{\circ}\text{C}$ . Most of these results showed unfavorable value of mobility ratio according Green and Willhite [47] since most of the value  $M > 1$ . In spite of this condition, as the viscosity of CO<sub>2</sub> increases, the mobility ratio decreases relatively to its gas phase at the respected temperature as shown in Table 4.5.

The temperature of  $T = 25^{\circ}\text{C}$  represent the temperature of core flooding. As shown in Table 4.5, it is evident that if core flooding is conducted at lower temperature would result in lower mobility ratio due to more viscous CO<sub>2</sub> injected. Lower mobility ratio is resulted in better displacement sweep efficiency because mobility ratio affects the stability of displacement process. Because mobility ratio is significant, a value of  $M < 1$  is a favorable mobility ratio [47]. The same condition can be observed in at CO<sub>2</sub> temperature of  $T = 20^{\circ}\text{C}$ ,  $12^{\circ}\text{C}$ , and  $5^{\circ}\text{C}$  where the mobility decreases as the temperature decrease.

Green and Willhite [47] explained that when one solvent is displacing a second solvent with which the first solvent is completely miscible and only one phase is flowing, the mobility ratio ( $M$ ) could be defined as the ratio of displaced fluid viscosity ( $\mu_d$ ) to the displacing fluid viscosity ( $\mu_D$ ). It means that this equation can be used when only two fluids exist within the porous medium.

By recalling the procedures in this experiment, there is still portion of water remaining in the porous medium before liquid CO<sub>2</sub> was injected. The mobility ratio calculated with Equation (9) is valid assuming that all the water that remains had been completely displaced by liquid CO<sub>2</sub>.

#### 4.2.4 Continuous Gas CO<sub>2</sub> Injection

This study also reported a result of Continuous Gas CO<sub>2</sub> Injection (CGI) EOR by using RPS-830. Although this section is not mentioned as scope of research, the purpose of conducting CGI CO<sub>2</sub> was merely for comparison purpose. The same initial condition was applied during crude oil saturation and water flood. For Continuous Gas CO<sub>2</sub> injection, the inlet pressure was maintained at 1500 psig (the same as experiment 7, 8, and 9) and core temperature was set to 40 °C to ensure the CO<sub>2</sub> injected was in gas state. The result of Continuous Gas CO<sub>2</sub> is shown in Figure 4.7 and Table 4.6.

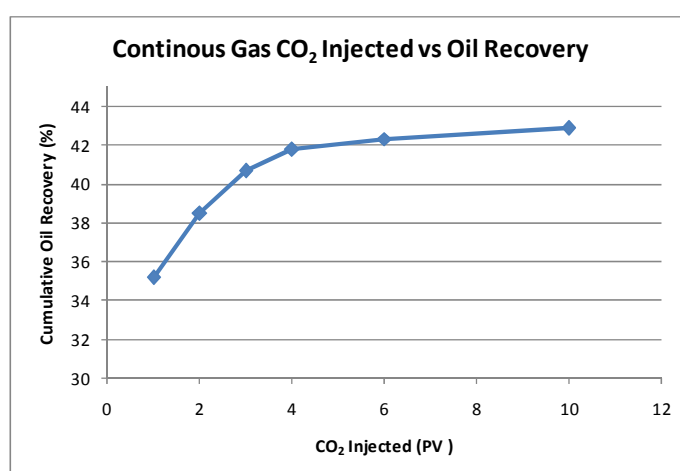


Figure 4.11 Cumulative oil recovery by injecting Gas CO<sub>2</sub> at 1500 psig and 40°C.

Table 4.6 Core flood injection profile and oil recovery by Continuous Gas CO<sub>2</sub> injection.

Exp. No.	$\phi$ (%)	OOIP (%PV)	Swc (%PV)	Water Injected (PV)	Water Flood Oil Recovery (% OOIP)	Sorw (%PV)	Total CO <sub>2</sub> Injected (PV)	Gas CO <sub>2</sub> Oil Recovery (%)
10	18.1	96.4	3.6	13.2	40.1	59.9	10	42.9

As shown in Figure 4.7 and Table 4.6, the injection of 10 PV gas CO<sub>2</sub> at pressure 1500 psig recover 42.9 % oil. Compared to experiment 7, 8, and 9 in Table 4.2 which have the same injection pressure, the result by liquid CO<sub>2</sub> injection were 67.7 %, 71.3 %, and 73.4 %. These results showed that liquid CO<sub>2</sub> injection gave significant improvement with more than 24 % difference in cumulative oil recovery. From the Appendix data of Jarrel [26], CO<sub>2</sub> viscosity at temperature of 40°C is 0.04879 cp. By applying the formula in Equation (9), the mobility ratio during this core flood experiment is 47.8.

Lower oil recovery during this experiment is resulted to the higher mobility ratio of the crude oil to the gas CO<sub>2</sub>. This condition stimulates the CO<sub>2</sub> to approach the outlet faster than liquid CO<sub>2</sub> before it has enough time to contact and displacing the crude oil within the porous medium.

By comparing experiment 7-9 in Table 4.3 with experiment 10 in Table 4.6, higher oil recovery of liquid CO<sub>2</sub> is resulted as the effect of mobility improvement and sweep efficiency to its liquid state. CO<sub>2</sub> gas tended to reach the sample end sooner because of its higher mobility thus less crude oil would be displaced. Meanwhile, at liquid state which had better viscosity, CO<sub>2</sub> gave relatively favorable sweep efficiency as to its gas state.

It is recognized that most process of gas displacing oil resulting in a very unfavorable mobility ratio that leads to poor microscopic sweep efficiency. This is the reason of immiscible gas injection is not really recommended as an EOR alternative [48]. Looking at the displacement mobility ratio at 40°C during continuous gas injection, CO<sub>2</sub> gas displacing a 2.33 cp crude sample at 1500 psig has a mobility ratio of 47.8, while CO<sub>2</sub> liquid displacement at this state is ranging between 28.5 until 20.8.

Although a mobility ratio of 28.5 is still high, it is a substantial improvement over the CO<sub>2</sub> gas displacement.

### 4.3 Measured Interfacial Tension between Crude Oil and CO<sub>2</sub>

The high pressure cell was first loaded with CO<sub>2</sub> at a pre-specified pressure and a constant temperature of  $T = 25^{\circ}\text{C}$ . Afterwards, oil sample was introduced into the pressurized cell by using pendant drop method. The results of IFT measurement between crude oil sample and CO<sub>2</sub> are displayed in Figure 4.8 and Table 4.7.

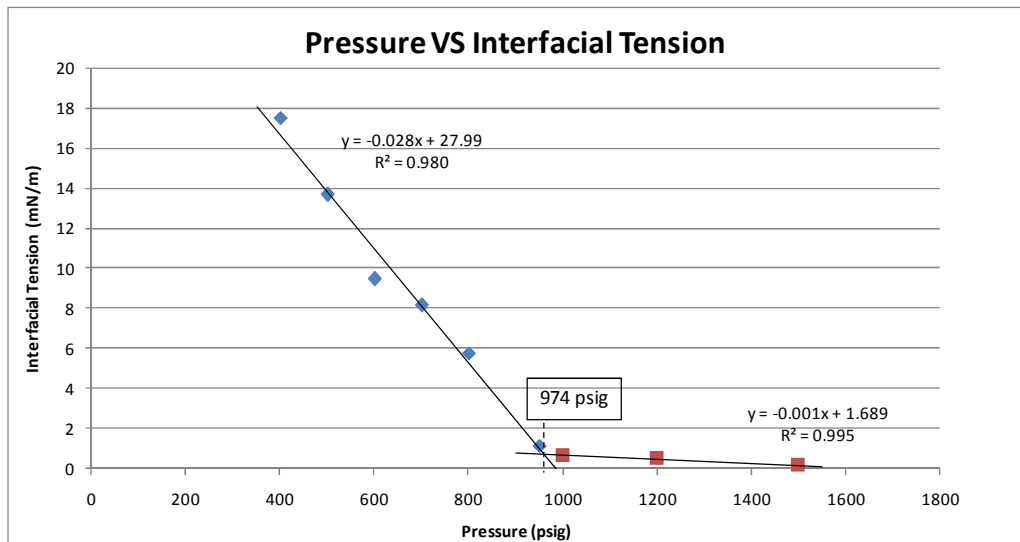


Figure 4.12 Measured interfacial tension of crude oil-CO<sub>2</sub> system at various pressure and  $T = 25^{\circ}\text{C}$ .

Table 4.7 IFT values measured between crude oil sample and CO<sub>2</sub> at different equilibrium pressures.

Pressure (psig)	IFT (mN/m)	
400	17.5	} Gas CO <sub>2</sub>
500	13.68	
600	9.45	
700	8.15	
800	5.79	
950	1.15	} Liquid CO <sub>2</sub>
1000	0.67	
1200	0.5	
1500	0.17	

From Figure 4.8, the IFT measurement results were almost linear with the constant pressure as long as the pressure was equal or lower than 974 psig. Figure 4.8 also displayed that once the pressure was higher than this threshold pressure, the IFT outcome become around 1 mN/m or even lower. In this case, escalating the pressure would give small effect to IFT reduction. The important threshold pressure from the equilibrium IFT versus equilibrium pressure curve is where the curve shows sharp change of slope [55] where the IFT is already low and approaching zero.

All IFT measurements below 1000 psig were conducted for 10 minutes with 1 second calculation interval. The oil drop tends to be stable during all measurement period because the system is fully closed during the entire measurement.

Meanwhile, at higher pressure, i.e. above 1000 psig, the measurement of oil-CO<sub>2</sub> IFT period could not be run more than 30 seconds. Drop volume and its shape changes faster as the measurement period increased because of the CO<sub>2</sub> started to miscible into crude oil. Measurement period more than 30 seconds would create poor drop shape to perform measurement which result no value displayed on the IFT outcome. This was attributed to the effect of CO<sub>2</sub> miscibility to crude oil which cause the drop shape became unstable and the volume of drop decreased and dissolved to surrounding system [56].

From IFT measurement results, it is known that at 950 psig, 1200 psig, and 1500 psig, the IFT between crude oil sample and CO<sub>2</sub> is approaching zero. Stalkup [10] mentioned that when interfaces between oil and displacing fluid is eliminated as a result from mixtures of miscible fluids, there are no IFT between the fluids which in this circumstance (the core flood experiment conditions), the IFT is very low and approaching zero.

#### **4.4 Liquid CO<sub>2</sub> Injection Limitations**

From the results and discussions previously, it is showed that liquid CO<sub>2</sub> injection method gave a satisfying increment in oil recovery. Liquid CO<sub>2</sub> injection offers an

alternative of enhanced oil recovery that could provide miscibility between CO<sub>2</sub> and crude oil with better displacement sweep efficiency.

However, there are some limitations in applying this method into the field scale projects. Since this method requires generating CO<sub>2</sub> in liquid state during displacement, the challenge is to find a reservoir with temperature lower than the critical temperature of CO<sub>2</sub> and withstand a pore pressure necessary to attain the liquid CO<sub>2</sub> without fracturing the reservoir.

Although this seems to be exclusive condition that might be rarely happens in oil field, nevertheless some of this exceptional fields have been investigated for the implication of liquid CO<sub>2</sub> enhanced oil recovery and published by Frailey et.al. [48] and Al-Quraini [49]. These mature fields are classified as Low Temperature Oil Reservoir (LTOR) and provide a unique opportunity for liquid CO<sub>2</sub> storage and its application as EOR method.

One of the fields investigated by Frailey et.al. [48] was Illinois Basin which covers the Indiana, Illinois, and Kentucky state in US. Data showed that the regional rule of thumb temperature gradient of Illinois Basin is 1 °F/100 ft and annual average temperature of 17°C at 100 ft below surface based on 40 years observation. For example, 21°C correspond to 900 ft and 31°C corresponds to 2700 ft. Based on these findings, it was concluded that the range of formation depths for liquid CO<sub>2</sub> flooding can be identified.

## CHAPTER 5

### CONCLUSIONS

The results of this thesis can be summarized as follow:

1. IFT between crude oil and CO<sub>2</sub> reduces as the equilibrium pressure increased until the value approach zero when the miscibility fully developed.
2. At flooding temperature of  $T = 25$  °C the estimated Minimum Miscibility Pressure by using the combination of Lasater and Holm-Josendal correlation is 671 psia.
3. Successful liquid CO<sub>2</sub> core flooding had been conducted by means of core flooding experiment with oil recoveries ranging from 24.7% to 73.4% after injecting 10 PV of liquid CO<sub>2</sub>.
4. Injecting liquid CO<sub>2</sub> into a porous medium produces higher oil recovery compared to the gas CO<sub>2</sub> when the displacement condition is above the MMP.
5. Increment in oil recovery by increasing the CO<sub>2</sub> injection pressure is higher compared to the increment in oil recovery by lowering the temperature of CO<sub>2</sub> injected.
6. The measured interfacial tension of crude oil sample and CO<sub>2</sub> system varied from 17.5 mN/m to 0.17 mN/m within the pressure range of 400 – 1500 psig and constant temperature of 25 °C.
7. The oil recovery by water flood in this study was in range of 36.1% until 39.7% after injecting 9 PV of brine into the core sample.

## **CHAPTER 6**

### **RECOMMENDATIONS**

The conclusion of the present study with respect to the research objectives can be summarized as follow:

1. In liquid CO<sub>2</sub> injection, slower injection flow rate, i.e. below 1 ml/min would represent the actual injection profile in the field. The flow rate of 1 ml/min or equal to 4.14 ft/day still excessive in 3 inch length core sample. Slower flow rate might escalate the injection period for the CO<sub>2</sub> to develop solvent bank and perfect miscibility.
2. Smaller interval of volume oil produced measurement is required for better precision in recovery development in every displacement phase.
3. Longer and bigger core sample dimension, i.e. 1 ft length and 3 inch diameter, might represent the precise solvent bank in the actual reservoir rather than shorter core.
4. The measurement of produced CO<sub>2</sub> by using gas collector would result in better understanding about the solubility of CO<sub>2</sub> in crude oil.

## REFERENCES

- [1] M.R. Todd, R.A. Slotbroom, and G.M. Bates, "Evaluation of A Tertiary Miscible Flood in the Keg River II Pool, Rainbow Field," *Petroleum Society of CIM*, June 1984.
- [2] S. Bagci and E. Tuzunoglu, "3D Model Studies of The Immiscible CO<sub>2</sub> Process Using Horizontal Wells for Heavy Oil Recovery," *The Petroleum Society*, June 1998.
- [3] Y. Zhang, X. Xie, and N.R. Morrow, "Waterflood Performance by Injection of Brine with Different Salinity for Reservoir Cores," , Anaheim, November 2007.
- [4] Energy Information Administration, "Country Analysis Brief: Malaysia," 2009.
- [5] M. K. Hamdan, N. Darman, and D. Hussain, "Enhanced Oil Recovery in Malaysia: Making it a Reality," *Asia Pacific Oil & Gas Conference & Exhibition*, April 2005.
- [6] Jr. Jennings and G. H. Newman, "The effect of Temperature and Pressure on the Interfacial Tension of Water Against Methane – Normal Decane Mixtureixtures," *SPE J*, 1971.
- [7] M. K. Masalmeh, "The effect of Wettability Heterogeneity on Capillary Pressure and Relative Permeability," *Journal of Petroleum Science and Engineering*, 2003.
- [8] W. Wang and Y. Gu, "Experimental Studies of Detection and Rouse of the Produced Chemicals in Alkaline-Surfactant-Polymer Floods," *SPE Reservoir Eval. & Eng*, 2005.

- [9] D.M. Wang, C.D. Liu, and G. Wang, "Development of an Ultra-Low Interfacial Tension Surfactant in a System No-Alkali for Chemical Flooding," , Tulsa, April 2008.
- [10] F. I. Jr Stalkup, *Miscible Displacement, SPE Monograph*. Richardson: Society of Petroleum Engineer, 1992.
- [11] N.J. Constant, *Improved Recovery Oil and Gas Production*, K.I. Stelzner, Ed. Austin, Texas, United States of America: Petroleum Extension Service Division of Continuing Education, 1983.
- [12] A. Farouq and S. Thomas, "The Promised and Problems on Enhanced Oil Recovery Methods," *J. Can. Pet. Tech.*, 1996.
- [13] R. K. Srivastava and S. S. Huang, "Technical Feasibility of CO<sub>2</sub> Flooding in Weyburn Reservoir - A Laboratory Investigation," *J. Can. Pet. Tech.*, 1997.
- [14] W. Barnhart and C. Coulthard, "Weyburn CO<sub>2</sub> Miscible Flood Conceptual Design and Risk Assessment," *J Can. Pet. Tech.*, 1999.
- [15] W. R. Brock, L. A. Bryan, and Exxon Co. U.S.A., "Summary Results of CO<sub>2</sub> EOR Field Test, 1972-1987," , Denver, 1989.
- [16] J. B. Magruder, L. H. Stiles, and T. D. Yelverton, "Review of the Means San Andreas Unit Full-Scale CO<sub>2</sub> Tertiary Project," *J. Pet. Tech*, pp. 638-644, 1990.
- [17] J. Prieditis, C. R. Wolle, and P. K. Notz, "A Laboratory Injectivity Study: CO<sub>2</sub> WAG in San Andreas Formation of West Texas," , Dallas, 1991, pp. 6-9.
- [18] C. Bardon and D. G. Langeron, "Influence of Very Low Interfacial Tensions on Relative Permeability," *SPE 53rd Annual Fall Technical Conference and Exhibition*, pp. 1-4, 1978.
- [19] J. F.R. Bellavance and Unocal Corp., "Dollahide Devonian CO<sub>2</sub> Flood: Project Performance Review 10 Years Later," , Midland, 1996.

- [20] D. Mangalsingh, T. Jagai, and SPE, "A Laboratory Investigation of the Carbon Dioxide Immiscible Process," , Port-of-Spain, 1996.
- R. E. Hadlow and Co. Exxon, "Update of Industry Experience with CO2
- [21] Injection," , Washinton, 1992.
- [22] P. Raimondi and M.A. Torcasso, "Distribution of Oil Phase Obtained upon Imbibition of Water," , Norman, 1963.
- [23] G. H. Thomas, G. R. Countryman, and I. Fatt, "Miscible Displacement in a Multihpase System," , Berkeley, 1983.
- [24] F. I. Stalkup, "Displacement of Oil by Solvent at High Water Saturation," , Tulsa, April 1969.
- [25] D. L. Tiffin and W. F. Yellig, "Effects of Mobile Water on Multiple-Contact Miscible Gas Displacements," , Tulsa, 1982.
- [26] P. M. Jarrel, C. E. Fox, H. S. Micheal, and L. W. Steven, *Practical Aspects of CO2 Flooding*. Richardson: Society of Petroleum Engineering, 2002.
- [27] E. C. Donaldson, *Enhanced Oil Recovery: Fundamentals and Analysis*. New York: Esevier, 1985.
- [28] Teknica, *Enhanced Oil Recovery*. Calgary: Teknica Petroleum Services Ltd., 2001.
- [29] J. W. Amyx, D. M.Jr. Bass, and R. L. Whiting, *Petroleum Reservoir Engineering Physical Properties.*: McGraw-Hill, 1988.
- [30] A. Danesh, *PVT and Phase Behavior of Petroleum Reservoir Fluids*. Edinburgh, Scotland: Elsevier, 1998.
- [31] E. A. Hauser and A. S. Micheals, "Interfacial Tension at Elevated Pressure and Temperature," vol. 52, no. 7, 1984.

- [32] E. W. Hough, M. J. Rzasa, and B. B. Wood, "Interfacial Tensions at Reservoir Pressures and Temperatures; Apparatus and the Water-Methane System," October 1950.
- [33] D. N. Rao and S. C. Ayirala, "The Multiple Roles of Interfacial Tension in Fluid Phase Equilibria and Fluid-Solid Interactions," in *Fourth International Symposium on Contact Angle, Wettability and Adhesion*, Philadelphia, 2004.
- [34] N. I. Kechut, M. Z. Zahidah, and Ahmad Noraini, "New Experimental Approaches in Minimum Miscibility Pressure (MMP) Determination," October 1999.
- [35] A. Firoozabadi and H.J. Ramey Jr., "Surface Tension of Water-Hydrocarbon Systems at Reservoir Conditions," *Journal of Chemical and Petroleum Technology*, May-June 1988.
- [36] J. C. Nicholas, *Oil and Gas Production Series: Improved Recovery*, Ione Stelzner Karen, Ed. Austin: The University of Texas Austin, 1983.
- [37] A. A. Zick, "A Combined Condensing/Vaporizing Mechanisms in the Displacement of Oil by Enriched Gas," in *SPE Annual Technical Conference and Exhibition*, New Orleans, 1986.
- [38] A. M. Elsharkawy, C. U. Suez, F. H. Poettmann, and R. L. Christensen, "Measuring Minimum Miscibility Pressure: Slim-Tube or Rising-Bubble Method?," in *Presented at the SPE/DOE 8th Symposium on Enhanced Oil Recovery*, Tulsa, April 1992.
- [39] J. Bon, SPE, and H. K. Sarma, "Investigation of Minimum Miscibility Pressure for CO<sub>2</sub>-Rich Injection Gases with Pentanes-Plus Fraction," , Kuala Lumpur, December 2005.
- [40] M. H. Holtz, V. N. Lopez, and C. L. Breton, "Moving Permian Basin Technology to the Gulf Coast, The Geologic Distribution of CO<sub>2</sub> EOR potential in Gulf Coast Reservoirs," , Midland, October 2005.

- [41] L.W. Holm and V.A. Josendal, "Effect of Oil Composition on Miscible-Type Displacement by Carbon Dioxide," *SPE/DOE Enhanced Oil Recovery Symposium*, November 1980.
- [42] L W Holm and V A Josendal, "Mechanisms of Oil Displacement by Carbon Dioxide," *Journal of Petroleum Technology*, 1947.
- [43] W. F. Yellig and R. S. Metcalfe, "Determination and Prediction of CO<sub>2</sub> Minimum Miscibility Pressures," *Journal of Petroleum Technology*, January 1980.
- [44] N. Mungan, "Carbon Dioxide Flooding – Fundamentals," *J.Cdn.Pet.Tech.*, 1981.
- [45] J. A. Lasater and Petroleum Co. Magnolia, "Bubble Point Pressure Correlation," *Fall Meeting of Southern California Petroleum Section*, October 1958.
- [46] O. M. Mathiassen, *CO<sub>2</sub> as Injection Gas for Enhanced Oil Recovery and Estimation of the Potential on the Norwegian Continental Shelf*. Trondheim: Norwegian University of Science and Technology, 2003.
- [47] D.W. Green and P.G. Willhite, *Enhanced Oil Recovery*, F.H. Poettmann and F.I. Stalkup, Eds. Richardson, Texas, United States of America: Society of Petroleum Engineers, 2003, vol. 6.
- [48] S. M. Frailey, J. P. Grube, and S. Beverly, "Investigation of Liquid CO<sub>2</sub> Sequestration and EOR in Low Temperature Oil Reservoirs in the Illinois Basin," , Tulsa, 2004.
- [49] A. Al-Quraini, Petroleum Development Oman, M. Sohrabi, and M. Jamiolahmady, "Heavy Oil Recovery by Liquid CO<sub>2</sub>/Water Injection," *SPE EUROPEC/EAGE Annual Conference and Exhibition*, June 2007.
- [50] E. Lindeberg, T. Holt, and IKU Petroleum Research, "EOR by Miscible CO<sub>2</sub> Injection in the North Sea," , Tulsa, April 1994.

- [51] D. M. Beeson and G. D. Ortloff, "Laboratory Investigation of the Water-Driven Carbon Dioxide Process for Oil Recovery," , Houston, October 1958.
- [52] R.H. Perry, *Perry's Chemical Engineer's Handbook; Seventh Edition*, D.W. Green, Ed. New York: McGraw-Hill, 1999.
- [53] E.J. Peters, *Petrophysics*. Austin, Texas: Department of Petroleum & Geosystem Engineering.
- [54] F.M. Perkins Jr., "An Investigation of the Role of Capillary Forces in Laboratory," *Society of Petroleum Engineering*, March 1957.
- [55] M. Nobakht, *Mutual Interactions between Crude Oil and CO<sub>2</sub> under Reservoir Condition*. Regina, Saskatchewan: University of Regina, 2007.
- [56] F.T. Chung, R.A. Jones, and H.T. Nguyen, "Measurements and Correlations of the Physical Properties of CO<sub>2</sub>/Heavy-Crude-Oil Mixtures," *SPE California Regional Meeting*, April 1986.
- [57] Teknica Petroleum Ltd., *Enhanced Oil Recovery*. Calgary: Teknica Petroleum Ltd., 2001.

**APPENDIX A**

**IFT MEASUREMENT PROCEDURE**

## **IFT Measurement Procedure**

The experiment procedures to measure IFT between CO<sub>2</sub> and crude oil in this study are listed as below:

1. Prior to each experiment, ensure that the cell and needle is cleaned by using tissue then flush it with compressed air.
2. Pressurize the cell with CO<sub>2</sub> to a pre-specified pressure by using one of the pressure generators. After the CO<sub>2</sub> is injected, it takes 15-30 minutes for the pressure inside the cell to reach the stabilized condition.
3. Introduce the crude oil by using crude oil sample cylinder which pressure is maintained between 15 psig to 75 psig higher than that of CO<sub>2</sub> phase inside the pressure chamber. The pendant oil drop is formed at the tip of the syringe needle, which is installed at the top of the high-pressure cell.
4. Generate a well shaped drop at the tip of the needle by opening the valve slowly.
5. Once this step is done, initiate IFT measurement at the specified equilibrium pressures.
6. For each acquired drop image, a high-precision calibration grid is used to calibrate the oil drop images and correct possible optical distortions. The output data also included the radius of curvature at the apex point, the surface area and volume of the pendant oil drop. Only the local gravitational acceleration and the density difference between the crude oil and CO<sub>2</sub> are required as input for this program.
7. The IFT measurement is repeated for at least three different pendant oil drops to ensure satisfactory repeatability at each pre-specified pressure and constant temperature. In this study, crude oil-CO<sub>2</sub> IFT were measured at constant temperature of 25°C and pressure range of 400 psig to 1500 psig.

## **APPENDIX B**

### **EXPERIMENTAL PROCEDURE FOR CORE FLOOD TESTS**

## Experimental Procedure for Core Flood Tests

The core flood test procedures in this study are listed as below:

1. Initially, saturate the core with brine for 8 by using manual saturator. Set the saturation pressure at 1200 psig to ensure the brine saturate all of pore spaces.
2. Take out the core from the saturator and attach the core into the core holder.
3. Prepare the injection fluid for each accumulator.
4. Set the initial overburden pressure to low condition and always maintain the overburden pressure higher than the core inlet pressure to prevent any back pressure effect from the core holder.
5. Initiate the injection procedure by injecting 100 ml brine into the core with flow rate 3 ml/min. The purpose of this step is to ensure that core is saturated with brine water.
6. Continue to crude oil injection with lower flow rate 0.8 ml/min to prevent the inlet pressure from increasing significantly. This is because the injected fluid is crude oil which has significant difference of viscosity compared to previous brine injected. The volume of crude oil injected is 200 ml.
7. When the flow is stabilized and the absent of brine produced on the collector, start injecting brine water flow rate of 3 ml/min. The volume of brine injected in this step is 150 ml.
8. Collect all the fluid produced during this injection with measuring tube. After all the brine had been injected, wait for additional 15 minutes and collect the oil produced as an effect of water injection.
9. Initiate liquid CO<sub>2</sub> preparation by compressing gas CO<sub>2</sub> in the accumulator along with temperature conditioning of the accumulator. The total volume of CO<sub>2</sub> accumulator is one liter. At 1,500 psig, this volume of gas CO<sub>2</sub> could produce around 170 ml of CO<sub>2</sub> liquid with the respected temperature range.
10. Once the accumulator pressure required is achieved, stop compressing and start the liquid CO<sub>2</sub> injection with 1 ml/min flow rate injection. Always regulate the backpressure valve to generate a stabilized injection pressure. Collect all the fluid produced intermittently. The average volume of CO<sub>2</sub> required in this step is 163 ml.

11. As soon as the liquid CO<sub>2</sub> injection phase is completed, stop the injection and release overburden pressure.
12. Remove the core sample and clean it by using toluene in Soxlet Extractor. The cleaning process requires at least 3 days to ensure no residual oil left in the pore space.
13. Before using same core sample for the second time, dry the core sample inside oven at 90°C for at least twelve hours to ensure the absent of toluene from the pore space.

**APPENDIX C**

**POROSITY MEASUREMENT PROCEDURE**

## **Porosity Measurement Procedure**

The experiment procedures to measure core sample porosity are listed as below:

1. Prepare the correct core holder size with the measured core dimension.
2. Install the core holder and connect PoroPerm with nitrogen tank and helium tank.
3. Key in the measured core dimension into the software interface and create a new recording file.
4. Run the porosity measurement and record the result.

**APPENDIX D**

**DENSITY MEASUREMENT PROCEDURE**

## **Density Measurement Procedure**

The experiment procedures to measure density of fluid are listed as follow:

1. Prepare the fluid that will be measured in a measuring glass.
2. Switch the portable density meter to On position.
3. Immersed the tubing bed below the surface of tested fluid.
4. Draw the tested fluid by pressing the button on top of the holder three times until all the measured fluid completely load the measuring tube.
5. Record the collected reading in the display.

**APPENDIX E**

**INITIAL WATER SATURATION PROCEDURE**

## **Initial Water Saturation Procedure**

The experiment procedures for initial core saturation are listed as below:

1. Load the saturator with brine in the beginning.
2. Place the core sample on the carrier plate and immerse both core sample and carrier plate into chamber that has been loaded with brine.
3. Closed the manual saturator and tight the connection.
4. Load the pressurizing container next to the saturator.
5. Increase the pressure inside manual saturator by pumping brine with the equipped lever until 1200 psig.

## **APPENDIX F**

### **MMP ESTIMATION OF LIQUID CO<sub>2</sub> CORE FLOOD EXPERIMENT**

### MMP Estimation Procedure

1. Crude oil specific gravity at standard condition (14.696 psia and 15.56 °C) is determined by using Equation (4).

$$\gamma = \frac{\rho_o}{\rho_w} = \frac{0.82}{0.998} = \mathbf{0.8216 \text{ gr/cm}^3}$$

2. Oil API degree of crude oil is determined by using Equation (5).

$$^{\circ}API = \frac{141.5}{\gamma} - 131.5 = \frac{141.5}{0.8216} - 131.5 = \mathbf{40.72^{\circ}}$$

3. The  $C_{5+}$  effective molecular weight of crude oil is determined by using Equation (3).

$$MW = \left( \frac{7864.9}{^{\circ}API} \right)^{\frac{1}{1.0386}} = \left( \frac{7864.9}{40.72^{\circ}} \right)^{\frac{1}{1.0386}} = \mathbf{158.84 \text{ lbmol}}$$

4. MMP of crude oil and  $CO_2$  by is determined by using Equation (2), at the respected temperature.

$$\begin{aligned} MMP &= -329.558 + (7.727 * MW * 1.005^T) - (4.377 * MW) \\ &= -329.558 + (7.727 * (158.84) * 1.005^{(77^{\circ}F)}) \\ &\quad - (4.377 * (158.84)) = \mathbf{671 \text{ psia}} \end{aligned}$$

**APPENDIX G**

**DATA OF OIL RECOVERY BY LIQUID CO<sub>2</sub> INJECTION**

### Oil recovery by liquid CO<sub>2</sub> at various injection profiles

P = 950 psig ; T = 20°C

Cumulative CO <sub>2</sub> injected		Cumulative Oil Produced	Recovery Factor
(ml)	(PV)	(ml)	(%)
10	0.6	1.6	16.8
30	1.8	2.1	22.1
50	3.0	2.2	23.2
100	5.9	2.3	24.2
170	10.1	2.3	24.2

P = 950 psig ; T = 12°C

Cumulative CO <sub>2</sub> injected		Cumulative Oil Produced	Recovery Factor
(ml)	(PV)	(ml)	(%)
10	0.6	1.7	18.7
30	1.8	2.2	24.2
50	3.0	2.5	27.5
100	5.9	2.6	28.6
170	10.1	2.6	28.6

P = 950 psig ; T = 5°C

Cumulative CO <sub>2</sub> injected		Cumulative Oil Produced	Recovery Factor
(ml)	(PV)	(ml)	(%)
10	0.6	1.7	18.7
30	1.8	2.3	25.3
50	3.0	2.7	29.7
100	5.9	3	33.0
170	10.1	3.2	35.2

**P = 1200 psig ; T = 20°C**

Cumulative CO <sub>2</sub> injected		Cumulative Oil Produced	Recovery Factor
(ml)	(PV)	(ml)	(%)
10	0.6	2.2	21.8
30	1.8	3.1	30.7
50	3.0	3.9	38.6
100	5.9	4.3	42.6
170	10.1	4.3	42.6

**P = 1200 psig ; T = 12°C**

Cumulative CO <sub>2</sub> injected		Cumulative Oil Produced	Recovery Factor
(ml)	(PV)	(ml)	(%)
10	0.6	2.3	23.2
30	1.8	3.4	34.3
50	3.0	4.2	42.4
100	5.9	4.6	46.5
170	10.1	4.7	47.5

**P = 1200 psig ; T = 5°C**

Cumulative CO <sub>2</sub> injected		Cumulative Oil Produced	Recovery Factor
(ml)	(PV)	(ml)	(%)
10	0.6	2.5	25.5
30	1.8	3.7	37.8
50	3.0	4.6	46.9
100	5.9	5	51.0
170	10.1	5.1	52.0

**P = 1500 psig ; T = 20°C**

Cumulative CO <sub>2</sub> injected		Cumulative Oil Produced	Recovery Factor
(ml)	(PV)	(ml)	(%)
10	0.6	3	32.3
30	1.8	4.6	49.5
50	3.0	5.7	61.3
100	5.9	6.2	66.7
170	10.1	6.3	67.7

**P = 1500 psig ; T = 12°C**

Cumulative CO <sub>2</sub> injected		Cumulative Oil Produced	Recovery Factor
(ml)	(PV)	(ml)	(%)
10	0.6	3.2	33.0
30	1.8	4.9	50.5
50	3.0	6	61.9
100	5.9	6.6	68.0
170	10.1	6.7	69.1

**P = 1500 psig ; T = 5°C**

Cumulative CO <sub>2</sub> injected		Cumulative Oil Produced	Recovery Factor
(ml)	(PV)	(ml)	(%)
10	0.6	3.2	33.7
30	1.8	5	52.6
50	3.0	6.2	65.3
100	5.9	6.8	71.6
170	10.1	6.9	72.6

### Summary of core flood experiment and calculation procedures

Exp. No. (1)	Core No. (2)	$\phi$		OOIP		$S_{wi}$ , ml (7)	Water Flood				
		ml (3)	% (4)	ml (5)	%PV (6)		Water Injected, ml (8)	Oil Recovery, ml (9)	Recovery Factor, % (10)	$S_{orw}$ , ml (11)	$S_{orw}$ , % (12)
1	2	16.84	19.4	15.3	90.9	1.54	150	5.8	37.9	9.5	62.1
2	2	16.84	19.4	15.1	89.7	1.74	150	6	39.7	9.1	60.3
3	2	16.84	19.4	15.2	90.3	1.64	150	5.9	38.8	9.3	61.2
4	3	15.38	17.7	14.9	96.9	0.48	150	5.6	37.6	9.3	62.4
5	1	15.76	18.1	15.5	98.4	0.26	150	5.6	36.1	9.9	63.9
6	1	15.76	18.1	15.5	98.4	0.26	150	5.5	35.5	10.0	64.5
7	2	16.84	19.4	15.1	89.7	1.74	150	5.7	37.7	9.4	62.3
8	3	15.38	17.7	15.0	97.6	0.38	150	5.6	37.3	9.4	62.7
9	1	15.76	18.1	15.0	95.2	0.76	150	5.7	38.0	9.3	62.0

(Continued)

Exp. No.	Liquid CO <sub>2</sub> Injection					
	Injection Pressure, psig (13)	CO <sub>2</sub> Temperature, °C (14)	CO <sub>2</sub> Injected, ml (15)	Oil Recovery, ml (16)	Recovery Factor, % (17)	$S_{or}$ , %OOIP (18)
1	950	5	168	3.2	33.7	66.3
2	950	12	168	2.4	26.4	73.6
3	950	20	168	2.3	24.7	75.3
4	1200	5	154	5.1	54.8	45.2
5	1200	12	158	4.7	47.5	52.5
6	1200	20	158	4.3	43.0	57.0
7	1500	5	168	6.9	73.4	26.6
8	1500	12	154	6.7	71.3	28.7
9	1500	20	158	6.3	67.7	32.3

The definition and calculation procedure of the table above:

- Column (3) and column (4) is core sample porosity which is resulted from laboratory measurement by using PoroPerm.
- Column (5) is resulted from the injection of core sample with crude oil by means of core displacement equipment until the absence of water produced at the outlet.
- Column (6) is the OOIP in term of % PV.

$$(6) = \frac{(5)}{(3)} \times 100\%$$

- Column (7) is the initial water saturation within the core sample after crude oil injection.

$$(7) = (5) - (3)$$

- Column (8) is the amount of water injected for water flood.
- Column (9) is the volume of oil recovered at the outlet after injecting the amount of water in column (7).
- Column (10) is the recovery factor of oil produced after water flood.

$$(10) = \frac{(9)}{(5)} \times 100\%$$

- Column (11) is the residual oil saturation after water flood in term of volume unit.

$$(11) = (5) - (9)$$

- Column (12) is the residual oil saturation after water flood in term of fraction.

$$(12) = \frac{(11)}{(5)} \times 100\%$$

- Column (13) is the inlet injection pressure of liquid CO<sub>2</sub>.
- Column (14) is the inlet injection temperature of liquid CO<sub>2</sub>.
- Column (15) is the volume of CO<sub>2</sub> injected into the core sample. This amount is equal to 10 PV to each core sample.
- Column (16) is resulted from the injection of core sample with liquid CO<sub>2</sub> in column (15) by means of core displacement equipment.
- Column (17) is the recovery factor of oil produced after liquid CO<sub>2</sub> injection.

$$(17) = \frac{(16)}{(11)} \times 100\%$$

- Column (18) is the residual oil in place after water flood and liquid CO<sub>2</sub> injection.

$$(18) = (5) - (11) - (16)$$

**APPENDIX H**

**DATA OF OIL RECOVERY BY GAS CO<sub>2</sub> INJECTION**

P = 1500 psig

; T = 40°C

Cumulative CO <sub>2</sub> injected		Cumulative Oil Produced	Recovery Factor
(ml)	(PV)	(ml)	(%)
15.8	1	3.2	35.2
31.5	2	3.5	38.5
47.3	3	3.7	40.7
63.0	4	3.8	41.8
94.6	6	3.85	42.3
157.6	10	3.9	42.9